Energinet.dk
ForskEl
FU 2007-1-7156

Final Project Report

Project full title: Quantify and Improve PEM Fuel Cell Durability
Grant agreement no.: FU 2007-1-7156

Project duration: 15-Mar-2010 to 31-Dec-2013
Project Coordinator: Laila Grahl-Madsen

Beneficiary no.	Beneficiary Name	Beneficiary short name	CVR
1 Coordinator	IRD Fuel Cells A/S Kullinggade 31 DK-5700 Svendborg	IRD	1468 9605
2	Department of Energy Conversion	DTU	3006 0946
3	Department of Chemical-Bio- and Environmental Technology	SDU	2928 3958

Contributors to the Final Report:

Laila Grahl-Madsen (IRD)
Jacob L. Bonde (IRD)
Niels J. Bjerrum (DTU)
Jens Oluf Jensen (DTU)
Qingfeng Li (DTU)
Lars N. Cleeman (DTU)
Shuang Ma Andersen (SDU)
Casper Frydendal Nørgaard (SDU)
Eivind Skou (SDU)

Final public project report!

SUMMARY AND CONCLUSION

The main objective of the DuRaPEM II project was to quantify and improve the durability of PEM FC's to enable the national target lifetimes to be met. Key issues on individual materials, single cells, and DMFC stacks was systematically addressed to establish a profound level of understanding and in this way improve the lifetime. The project approach and main scientific targets are summarised below:

- Obtain fundamental understanding of degradation mechanisms and utilise this knowledge to reduce the voltage decay rate
- Refinement of accelerated test matrix and apply results to a lifetime model
- Control the electrochemical solubility of the precious catalyst to extend lifetime and enable regeneration of catalyst at the EoL (End-of-Life)
- Optimize the operating conditions in order to improve lifetime and demonstrate improved lifetime on single cells (LT PEM, DMFC & HT PEM) and stacks (DMFC)

The project was initiated in Mar-10 and completed in Dec-13. The LT & HT PEMFC activities are continued in the already on-going DuRaPEM III project (ForskEl 2013-1-12064). The consortium consists of three (3) partners with the following complementary activities:

- IRD Fuel Cells A/S [IRD], responsible for the following:
  - Project coordination
  - LT PEM & DMFC MEA manufacture for the SDU and the IRD experimental work
  - LT PEM FC single cell test
  - DMFC FC single cell and stack test
  - Membrane AST test
- Department of Chemical- Bio- and Environmental Technology [SDU] being main responsible for the following
  - Ex-situ and in-situ precursor test
  - Development of a method to re-utilise the catalyst precursor
- Department of Energy Conversion and Storage **[**DTU**]** being main responsible for the following:
  - HT PEM FC ex-situ precursor tests, mainly membrane test
  - HT PEM FC single cell test
  - HT PEMFC post mortem characterisation

Carbon nanofiber (CNF) and carbon nanotube (CNT) supported platinum catalysts were prepared and optimized. The catalysts were evaluated with respect to thermal and electrochemical stability with traditional carbon black (Vulcan) based catalyst as reference. From carbon thermal stability, decomposition, electrochemical degradation in acidic aqueous media and cyclic voltage treatments, both carbon nanofiber and carbon nanotube demonstrated better stability than carbon black. High crystalline CNF showed a higher stability than CNT during the entire measurements. Single cell tests with MEAs prepared with CNF or CNT supported catalysts did not show improved BoL performance, but better durability than MEAs equipped with electrodes based on the SoA carbon-black supported catalysts. CNF & CNT based platinum catalyst PEM fuel cells could therefore provide a more durable and more stable power source. Optimization and activation of the MEA electrode structure is the key point to gain better cell performance for carbon nanomaterials.

Table 1 The national Danish LT PEMFC road map targets and the corresponding acceptable cell voltage decay rate using a 10% voltage loss as an End-of-Life (EoL) definition.

	Single cells		Stacks aimed for stationary applications	
	Lifetime	Corresponding acceptable voltage decay rate	Lifetime	Corresponding acceptable voltage decay rate
2012	10,000 h	7 µV/h	6,000 h	12 µV/h
2014	12,000 h	6 µV/h	10,000 h	7 µV/h
2016	15,000 h	5 µV/h	12,000 h[i]	6 µV/h
2020	50,000 h	1.4 µV/h	30,000 h	2 µV/h

Platinum metal can be dissolved electrochemically and subsequently re-deposited as nanoparticles on a carbon substrate, without intermediary separation and handling of pure platinum salt. This enables circumvention of the emissions of ammonia, chlorine, hydrogen chloride and nitrogen dioxide associated with conventional processes for recycling of platinum catalyst from polymer electrolyte fuel cell electrodes. Practical challenges remain for its application as a recycling scheme for platinum catalyst from polymer electrolyte fuel cells, relating to the sustainment of electrical contact to the platinum during electrolysis.

Two (2) types of LT PEMFC MEAs have been long-term tested. One set of MEAs were equipped with ordinary IRD Pt/Ru anodes that are capable of reformate operation, the other set of tested MEAs are equipped with pure Pt-anodes. The purpose was to investigate the Ru-alloy catalyst stability on the anode. All the other MEA precursors are identical for all five (5) MEAs. The MEAs have been exposed to two different load densities (0.33 A/cm^2 or 0.66 A/cm^2). The cells are operated on constant load for 250 hours and then electrochemically characterised (IV, H_2 crossover, ECSA etc.). None of the MEAs showed any increase in the hydrogen crossover even after more than 10,000 hours of operation. The cathode ECSA decreases significantly for all MEAs during the first 2,000 hours of operation. The loss of catalytic surface area after this point is minor. Experimental difficulties with all three (3) MEAs having pure Pt-anodes have occurred. However, the indication is that the investigated MEAs perform equally well. The overall degradation rate observed for all MEAs decreases continuously with increasing operation time, starting at very high levels (>100 µV/h). The high initial degradation is caused by catalyst growth, particularly at the cathode. The main precursor focus for lifetime improvements should therefore be put on the cathode catalyst. The decay rate observed at steady state operation is significantly higher for all MEAs than the decay rate obtained from the I-V characterisations. It is therefore concluded that the irreversible degradation is acceptable, but can be improved particularly by improving the cathode catalyst. The lowest irreversible degradation rate is 1 µV/h, which corresponds to a lifetime of 70,000 h. This is better than the 2020 Danish Road Map target for MEAs (Table 1).

Four (4) DMFC single cells has been long term tested (in total for 27,600 test hours) under controlled environment in the laboratory. Three (3) different test protocols has been applied. The main difference between the protocols is related to the length and frequency of the refresh cycles that implies current interruption. The results show that the best MEA possessed an average degradation rate of 8.5 µV/h over the 8,773 hours tested. This is well in-line with the national

[i] The listed Road Map targets is 20,000 h's of lifetime, which cannot be true as the target cell lifetime is shorter (15,000 h)

Table 2 The national Danish DMFC road map targets and the corresponding acceptable cell voltage decay rate using a 10% voltage loss as an EoL definition.

	Single cells		Stacks	
	Lifetime	Corresponding acceptable voltage decay rate	Lifetime	Corresponding acceptable voltage decay rate
2012	5,000 h	8 µV/h	2,000 h	20 µV/h
2014	6,000 h	7 µV/h	5,000 h	8 µV/h
2016	8,000 h	5 µV/h	6,000 h	7 µV/h
2020	10,000 h	4 µV/h	7,500 h	5 µV/h

Danish road-map lifetime target for 2012 which is 8 µV/h[ii] (Table 2). The other tested MEAs possessed higher degradation rates ranging from 12 to 16 µV/h. The intermediate characterisations illustrate a significant loss of cathode ECSA (≈35%), but no significant membrane crossover development nor anode catalyst coarsening. The MEAs have after EoT been characterised for microstructural changes (SEM) and element redistribution (EDX) at the Danish Technological Institute. The microstructural characterisation show a significant alteration of the cathode that are markedly thinned and locally totally corroded/missing. Traces of Ruthenium is detected on the cathode, showing that MeOH and Ru crossover from the anode towards the cathode goes hand-in-hand. A significant Ru-depletion is detected on the anode air-inlet location. The obtained results have been used to successfully optimise the operational strategy of IRDs DMFC-module.

Overall the DMFC stacks have been operated ≈7,500 hours in total in the period of the project. One stack has been operated for 3,600 hours with an cell average degradation of 14 µV/h. Analysis of the stack that operated 3,600 hours showed that MEA's in one of the two fuel circuits possessed a degradation of 8.1 µV/h on average, this exceed the national roadmap targets for 2012 and almost reaches the 2014 roadmap targets for stacks (Table 2).

A single cell test matrix with 17 experiments has been completed for the HT PEMFC track. The overall goal was partly to establish a performance and durability baseline and partly to determine the influence of the individual operational parameters. The test matrix was completed for both 20 and 40 µm thick membranes. The durability matrix gave the following conclusions

- Under steady state conditions the main degradation comes from the membrane. The membrane degradation is not constant, but accelerates close to EoL
- Catalyst degradation is mainly observed during start and stop cycling
- Biggest improvement in durability has come from improvement in manufacturing of the existing MEAs
  - Higher uniformity of the membrane results in longer lifetime. During the project the MEAs produces have seen a significant improvement in membrane thickness variations from ±10 µm, down to ±2 µm with can be directly read in the durability of the MEAs
  - Control of doping level improve durability
  - Better control of the assembly procedure for the MEAs has also results in improved durability
- Acid management is key to improve the membrane performance
- Running at higher current densities significantly decreases durability

[ii] No lifetime target is defined for 2013

Overall, the project has resulted in a better understanding of the HT PEMFC degradation mechanisms, primarily the main degradation mechanism being the loss of ionic conductivity over time.

The dissemination activities within the project has been good, nine (9) papers in peer-reviewed papers have been published, one (1) patent is drafted, 11 oral and/or posters have been presented, and one book chapter has been made.

TABLE OF CONTENT

1. INTRODUCTION

1.1 PREFACE

The present project is a continuation of the PSO project "Quantify and Improve PEM Fuel Cell Durability, Part I" (FU 2007-1-7156) that was terminated in May-2010. The work on quantifying and improving the durability and lifetime of PEMFC continues in the already on-going Project Part III that also is supported by PSO through contract 2013-1-12064.

1.2 PROJECT OBJECTIVES

The main objective of the DuRaPEM project was to develop a pathway and technology for PEM FC's enabling the national target lifetimes to be met. The project approach was systematically to quantify and improve the durability of PEM FC's.

The project approach and main scientific targets are summarised below:

- Obtain fundamental understanding of degradation mechanisms and apply these in order to reduce the voltage decay rate
- Refinement of accelerated test matrix and apply results to a lifetime model
- Control the electrochemical solubility of the precious catalyst to extend lifetime and enable regeneration of catalyst at the EoL[iii] (End-of-Life)
- Optimize operating conditions in order to improve lifetime and demonstrate improved lifetime on single cells (LT PEM, DMFC & HT PEM) and stacks (DMFC)

The reported project is a continuation of the completed ForskEl project "Quantify and Improve PEM Fuel Cell Durability" (PSO-2007-1-7156), through which fundamental understanding and identifying of key issues for both LT-PEM FC, DMFC and HT-PEM FC durabilities was achieved. The factors affecting performance degradation have gradually been recognized. New challenges have been encountered and some of the bottlenecks for improving the durability have been identified. However, more systematic data was essential in order to narrow the gap between today's status and the required market targets for lifetime and cost.

The present project was directed at systematically addressing these key issues from the individual materials to the stack level and in doing so establishing a profound level understanding with respect to optimised materials and technologies that improves durability.

1.3 *STATE-OF-THE-ART* AT PROJECT START

Owing to their high energy efficiency, convenient operation, and environmentally friendly characteristics, PEMFCs are considered one of the most promising fuel-cell technologies for both stationary and mobile applications. Significant progress has been achieved over the past few decades. However, durability and cost have been identified as the top-two issues for PEMFC technology. To reach technological readiness stationary fuel-cell systems must meet durability targets of at least 40,000 h (≈4.5 years of continuous operation) in order to compete with existing distributed-power-generation systems. The national Danish durability targets for stationary fuel-cell applications stand on the lifetimes of energy conversion devices that are competitive with fuel cells.

[iii] Abbreviations are listed in Section 8, *ibid*

However, currently the lifetimes of LT-PEMFC stationary cogeneration systems are ≈10,000 h[1], and in the same order of magnitude for HT-PEMFC single cells[2,3&4]. Clearly, intensive R&D is still needed to address the issues related to PEMFC durability and degradation rates in order to achieve sustainable commercialisation.

To date, various failure modes have been identified, for example, catalyst particle ripening (particle coalescence), preferential alloy dissolution in the catalyst layer, carbon-support oxidation (corrosion), catalyst poisoning, membrane thinning and pinhole formation, loss of active acid groups in the ionomer phase of the catalyst layer and/or in the membrane, bipolar plate surface film growth, hydrophilicity changes in the catalyst layer and/or gas diffusion layer (GDL), and PTFE decomposition in the catalyst layer and/or GDL.

1.3.1 LT PEM FC

The main technical barrier for the acceptance of fuel cells as a practical power source is durability under a wide range of operational conditions. For different applications, the requirements for fuel cell lifetime vary significantly, ranging from +5,000 h for cars to +40,000 h of continuous operation for stationary applications. Unfortunately, at present most PEM fuel cell provided by manufacturers and research institutes cannot achieve these goals. Selected results on continuous operation reported in the literature are shown in Table 3. Most results show encouraging degradation rates indicating much longer lifetime than actually tested, one test period exceeds the academic EoL criterion[iv]. However, it is not clear in the literature whether the reported results represent reversible or the irreversible decay rates.

Table 3 Literature summary compiled by Wu et al. (2008)[5] of steady state LT PEMFC lifetime tests.

Authors (cf. Wu et al. 2008)[5]	**Test time (h)**	**Degradation rate [µV/h]**	**Corresponding lifetime (ΔU = -10%)**
Ralph	5,000	4	10,000 h
St-Pierre et al.	5,000	1	40,000 h
Washington	4,700 8,000	6 2.2	6,667 h 18,182 h
Endoh et al.	4,000	2	20,000 h
Yamazaki et al.	8,000	2–3	-
St-Pierre and Jia	11,000	2	20,000 h
Fowler et al.	1,350	11	3,636 h
Ahn et al.	1,800	>4,000	-
Cheng et al.	4,000	3.1	12,903 h
Scholta et al.	2,500	20	2,000 h
Cleghorn et al.	26,300	4–6	-

[iv] EoL obviously occurs when a MEA in a FC stack cannot perform any longer (min. $U_{Cell} \leq 0$ V). However, EoL occurs at an earlier stage than at total failure. The generally accepted academic definition on EoL, and the one used within this report, is defined as a voltage loss of 10% at rated power.

Table 4 Summary of durability results for PBI based HT-PEMFC reported by various groups.

Overall degradation of PBI cells under steady state operation with H_2 and air at 150-160ºC	
DTU-ECS & DPS	>5,000 h at 150ºC; degradation rate <5 µV/h <2,000 h at 180-200ºC
BASF-PEMEAS	>20,000 h at 160ºC; degradation rate 5-6 µV/h
Plug Power	Degradation rate of ≈12 µV/h at 0.2 A/cm^2
Sartorius	2 kW PBI stack at 160ºC; degradation rate <10 µV/h
Juelich	>6,000 h at 160ºC; degradation rate≈ 25 µV/h
FuMa-Tech	10,000 h at 150ºC; degradation rate <5 µV/h
Dynamic lifetime tests of PBI cells	
DTU-ECS & DPS	H_2/Air, daily cycling RT&150ºC, 860 cycles, 3.5 years degradatio rate ≈300 µV/cycle
BASF-PEMEAS	H_2/Air, daily cycling RT&160ºC, 260 cycles, 6,500 h, 300 µV/cycle or 11 µV/h
Volkswagen group	H_2/Air, 2h/2h cycling 40&160ºC, >600 cycles in 2,500 hours: ≈183 µV/cycle

1.3.2 DMFC

To date, various failure modes in LT PEMFC have been identified, i.e. catalyst particle ripening (particle coalescence), preferential alloy dissolution in the catalyst layer, carbon-support oxidation (corrosion), catalyst poisoning, membrane thinning and pinhole formation, loss of active acid groups in the ionomer phase of the catalyst layer and/or in the membrane, bipolar plate surface film growth, hydrophilicity changes in the catalyst layer and/or gas diffusion layer (GDL), and PTFE decomposition in the catalyst layer and/or GDL. Many of these failure modes are also valid for DMFC, but this PEM-variant has some additional challenges e.g. MeOH & Ru-catalyst crossover. The published knowledge on DMFC durability is limited. Fletcher & Cox (2011)[6] reported a DMFC MEA degradation rate of 16 µV/h after ≈2,750 test hours, while Chin et al. 2010[7] reported a voltage decay ≤20% within the tested 1,000 hours. These degradations are more than twice as high as the defined acceptable MEA degradations in the national Danish road map for 2012.

1.3.3 HT PEM FC

HT-PEMFC has reached a reasonably mature state of development in terms on both power performance and durability (Table 4).

The steady state operation with a constant load is a mild operational mode for PBI cells. First of all, no liquid water formation is involved at 150-160°C. This minimizes the risk of acid washing out, which has been a critical concern for acid based PBI fuel cells. Another feature of this operational mode is that the cell voltage always remains in the low range, which minimizes the oxidation of both carbon supports and noble metals and therefore the catalyst degradation. It is clearly seen from the table that lifetime in the range of 5,000 to 20,000 hours has been achieved under steady state operation with H_2 and air at 150-160ºC. Under these conditions a typical degradation rate is about

Table 5 List of Milestones.

ID	WP	Title	Nature
MS1	1	Experimental test matrix for LT-PEM and DMFC completed	Report
MS2	1	Experimental test matrix for HT-PEM completed	Report
MS3	2	MEA separation techniques developed	Report
MS4	3	Report on model for LT-PEM MEA lifetime prediction	Report
MS5	4	Report on model for DMFC MEA lifetime prediction	Report
MS6	5	Strategic concepts for overall durability improvement	Report
MS7	5	Optimised polymer membranes available for MEA fabrication	Report
MS8	5	Optimised catalysts with modified/alternative supports available	Sample
MS9	2	Catalyst recovery demonstrated	Report
MS10	2	Process to fabricate catalyst powder from re-used metals identified	Report
MS11	3	Report on optimised LT-PEM operation	Report
MS12	4	Report on optimised DMFC components and stack operation for WP4.5	Report
MS13	2	Fabrication of generated catalyst for test completed	Component
MS14	3	Conclusion on accelerated test and lifetime model for LT-PEM	Report
MS15	4	Conclusion on accelerated test and lifetime model for DMFC	Report
MS16	5	New MEA evaluation results	Report
MS17	0	Four papers submitted to international journals with peer review	Report
MS18	2	Compiled evaluation on catalyst lifecycle	Report
MS19	3	Report on long-term LT-PEM MEA test	Report
MS20	4	Report on 3,000 hours DMFC stack test	Report
MS21	5	Operational strategy for HT-PEMFC	Report

5-10 µV/h, which can be translated to a service life of 12,000 hours if the cell death is defined as 10% loss of the initial cell voltage (say from 0.6 V).

During dynamic tests with thermal, load and shutdown-start up cycling, the amount and the vapour pressure of the water produced varies and formation of liquid water might be involved. In addition, the shutdown-start up or/and temperature cycling causes thermal and mechanical stresses to catalyst layers, membranes and their interfaces as well as the volume expansion and contractions of the acid in MEAs. Another important mechanism of the cell degradation involved in these dynamic tests is the corrosion of carbon support and sintering of noble metal catalysts when the cathode is exposed to high or open circuit potential. Under dynamic mode, it is no surprising that a much faster degradation is observed. The DTU-ECS & DPS team has performed a daily start-stop test in an overall period of 3.5 years with an accumulated operating time of 6,000 hours[2]. The observed degradation rate is about 300 µV for every shutdown/start up cycle. The BASF group observed a very similar rate while the Volkswagen group reported a slightly lower rate (183 µV/cycle) with both a shorter cycle and a smaller temperature range.

1.4 PROJECT OVERVIEW

The original project was scheduled for three (3) years, but has been extended to 46 month. The original defined Gantt including WP-leaders (main actor) is shown in Fig. 1. The defined milestones for the project are listed in Table 5. There have been some changes in the milestone responsibilities as follows:

- IRD and SDU was originally jointly responsible for MS18: Compiled evaluation on catalyst lifecycle. SDU has solely taken over this responsibility.
- DTU and IRD was originally jointly responsible for MS21: Operational strategy for HT-PEMFC. DTU has solely taken over this responsibility.

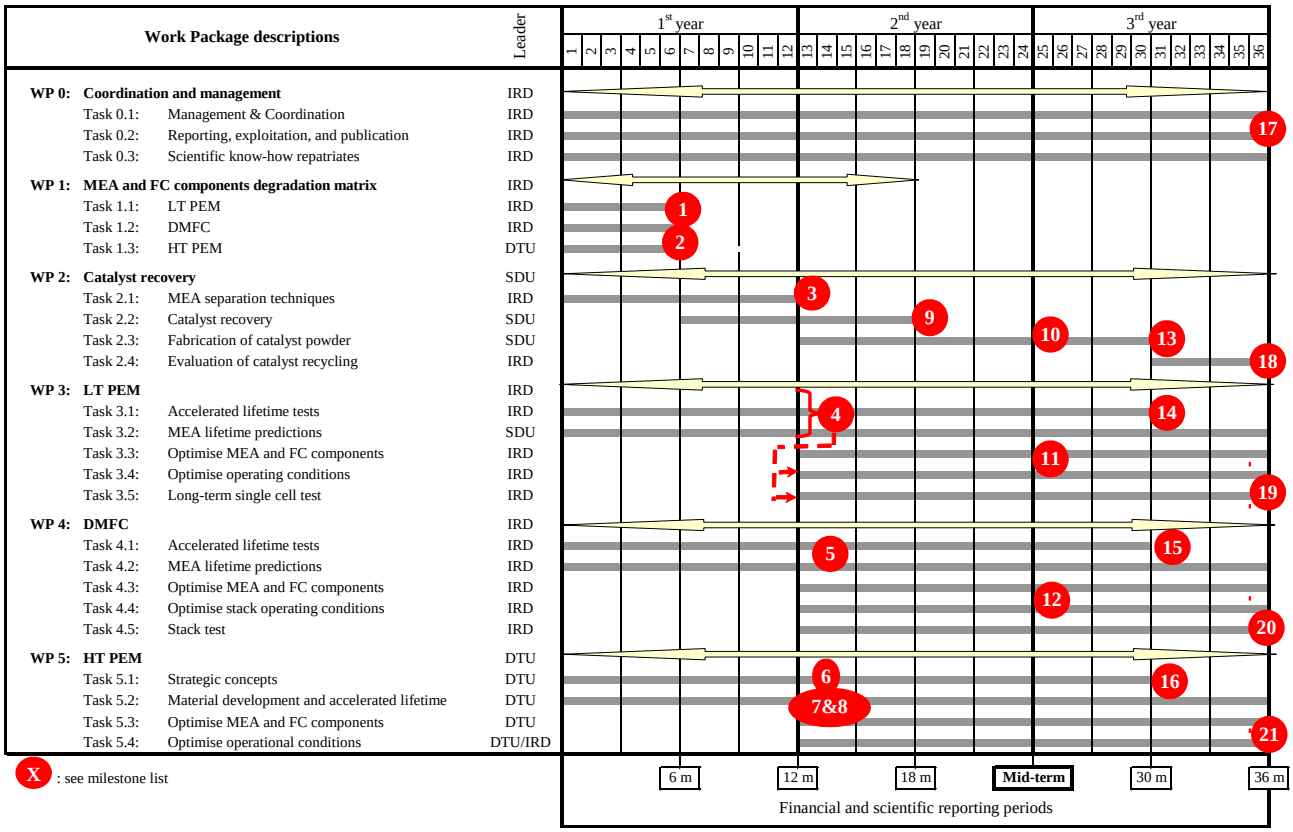

Fig. 1 Project Gantt; milestones (cf. Table 5) are indicated with circular red symbols.

2. LT PEM & DMFC PRECURSORS

2.1 INTRODUCTION

Proton exchange membrane fuel cells (PEMFC) have been received significant development in the past decades as one of the main alternative power sources for stationary and mobile applications because of their high-power density, low weight, simplicity of operation, high-energy conversion efficiency, and zero harmful emissions. The PEMFC stacks with electric powers of 1 kW, 2 kW, 5 kW, and 10 kW have been developed in different countries. However, the cost of PEMFC stacks is still far too high for many applications. One of the major obstacles for the broader commercialization of PEMFC is the high cost of catalysts. The effort to reduce cost has so far been focused on cheaper precursors, performance improvement, and minimizing labour in the FC-stack manufacture by rationalising the production. Good progress has in these matters been obtained, but substantial further cost reduction has to include the recycling perspective. The approach to reduce cost within DuRaPEM II has been to develop an alternative approach to platinum recycling from discarded fuel cell membrane-electrode-assemblies. The idea is to bring platinum into solution electrochemically, thus avoiding the consumption of bulk chemical oxidizing agents and the associated emissions to air. Furthermore, the intention is to limit the need for purification of platinum from the acid medium by re-precipitating platinum as nanoparticles on fresh carbon substrate immediately from the acid solution with minimal pre-treatment.

The work within DuRaPEM II also includes ex-situ tests of other precursors, particular AST membrane tests.

2.2 CATALYST

Among numerous chemical, mechanical and thermal degradation challenges, loss of noble metal catalyst and consequently decline of cell performance due to instability of the supporting carbon (carbon corrosion) is one of the important failure modes for PEMFCs. Moreover, the degradation of carbon support and catalytic metals interact with and exacerbate one another. On the one hand, oxidation of carbon is promoted by the platinum particles due to their catalytic effect; on the other hand, once the carbon supports are corroded, the catalysts lose their physical support, electrical contact, balanced electrode structure, and consequently an overall decreased electrochemical active surface area[8-9]. Therefore, a stable support is one of the key components for a stable catalyst in PEMFC. Carbon nanofiber (CNF) and carbon nanotube (CNT) supports are receiving more and more attention due to their impressive thermal, mechanical and electric properties in various areas[10]. Their potentials were especially exploded within fuel cell application and hydrogen storage[11-12] in the last ten years

In the following session, CNT and CNF as alternative platinum catalyst supports for Proton Exchange Membrane Fuel Cells (PEMFCs) were assessed. Platinized CNF and CNT using a standard polyol method were prepared and fabricated as cathodes of Membrane Electrode Assemblies (MEA) for PEMFC. Both the catalysts as such and the MEAs made out of them were evaluated regarding to thermal and electrochemical stability using traditional carbon black (Vulcan XC72) as a reference. Carbon surface properties, thermal corrosion at constant temperature, thermal gravimetric analysis (TGA), cyclic voltammetry (CV), polarisation curve, and impedance spectroscopy were applied on the samples under accelerated stress conditions.

Major observation, example of Fig. and summary are included in the present report. Experimental details and results can be found in the publication Andersen et al. (2013), cf. section 6.

Table 6 List of carbon and carbon supported catalyst information

No.	Name	Element content	Catalyst wt%	Alloy ration	Carbon type	Catalyst or carbon diameter nm	Surface area m^2/g
1	CNF	C	0	-	CNF	150	13
2	CNT	C	0	-	CNT	15	270
3	Vulcan XC-72	C	0	-	Vulcan	~13	209
4	Ketjenblack	C	0	-	HSCB	~2	1,421
5	CNF 20% Pt	Pt/C	20	-	CNF	2.79	10.5
6	CNT 20% Pt	Pt/C	20	-	CNT	3.10	90.4
7	Vulcan 20% Pt BASF	Pt/C	20	-	Vulcan	2.50	112
8	Hispec 9000	Pt/C	57.84	-	Vulcan	5.47	103
9	Hispec 9100	Pt/C	56.76	-	*	2.77	305
10	Hispec 10000	PtRu/C	59.72	1:1	Vulcan	2.90	114
11	Hispec 10100	PtRu/C	58.61	1:1	*	2.28	287
12	Blank	-	-	-	-	-	-

* Hispec 9100 and 10100 are using the same type of carbon support, however the detail is confidential

2.2.1 CATALYST EX-SITU TEST

Due to the emergence of vast amount of catalyst for PEMFC application with the accelerated technology development, first phase ex-situ evaluation is one of the indispensable steps for a fast screening and comparison of promising catalyst candidates. A complete list of the catalysts that have been studied is listed in Table 6.

2.2.1.1 Surface properties characterization (SEM and TEM)

VGCF™ (CNF herein) are vapour grown highly graphitized carbon nanofibers with an average diameter of 150 nm, whereas VGCF-X™ (CNT herein) are multi-walled carbon nanotubes with an average diameter of about 15 nm. Their SEM morphology is shown in Fig. 2A. Dispersed Pt nano-particles of very small and uniform size distribution (2-3 nm) were obtained on both carbon supports, as shown in the TEM images in Fig. 2B for Pt/CNF and Pt/CNT respectively.

2.2.1.2 Thermal stability

CNF & CNT and traditional carbon black demonstrate clear different degradation patterns. Both CNF and CNT based catalysts showed less than 10% carbon weight loss, while one commercial carbon showed between 78 to 88% weight losses. Vulcan based catalysts showed 24-55% weight loss depending on the catalyst loading and the catalyst properties: The higher the platinum content, the more vulnerable of the carbon; PtRu type catalyst is seen more efficient in catalysing carbon corrosion. CNF and CNT based catalysts, carbon degrades very similarly. Moreover, both of them are superior to Vulcan based catalysts (BASF and Johnson Matthey).

2.2.1.3 Thermal decomposition (Thermogravimetry)

One example of the weight changes of destructible material (carbon and Nafion ionomer) in the sample mixture determined by thermogravimetry is shown in Fig. 3. The major turning point in the curve is well recognized combustion of carbon which came from the destruction of the crystal structure during the experimental process, and the minor turning point at lower temperature is due to decomposition of the organic polymers (Nafion ionomer).

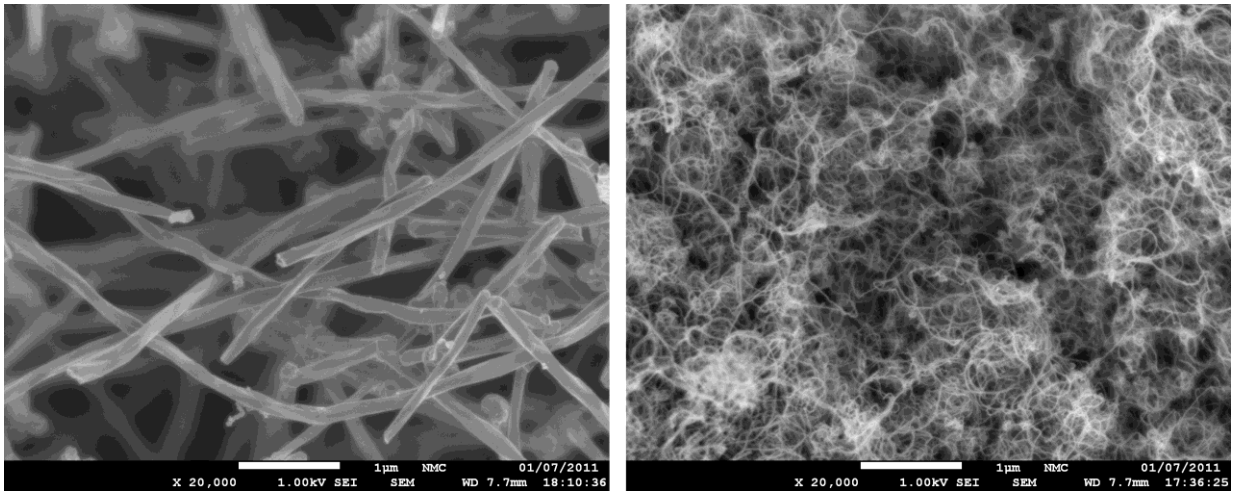

A

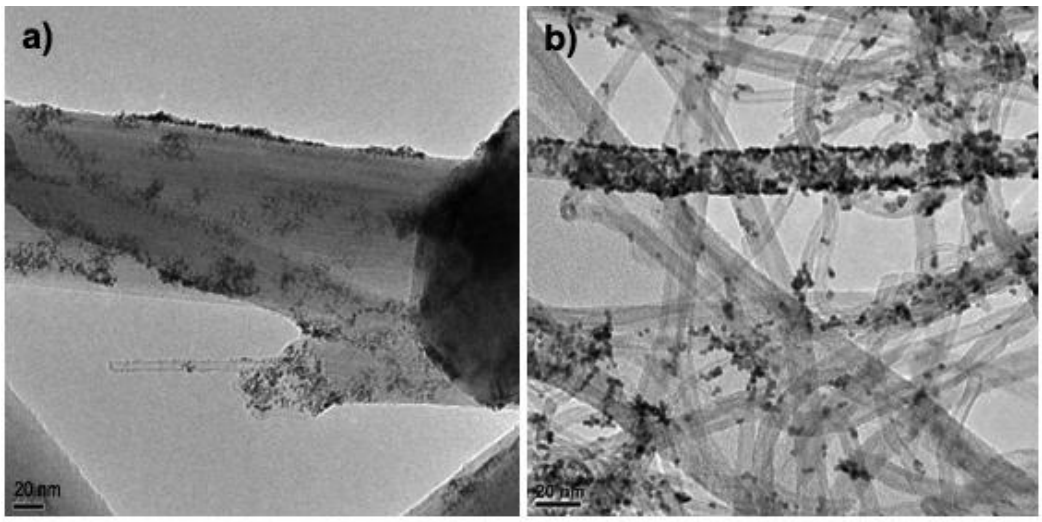

B.

Fig. 2 A: SEM images of the catalyst carbon supports: (a) CNF and (b) CNT
B: TEM images of Pt deposited on: (a) CNF and (b) CNT

For all the three types of carbons, when they are finely "mixed" with either platinum or Nafion ionomer or both of them, their decomposition temperatures (DT) decrease with different extent. In general, it demonstrates that nanosized platinum is very effective in catalysing carbon decomposition, as mentioned at 2.2.1.2 as well; moreover, introducing Nafion ionomer contributes also carbon degradation.

2.2.1.4 Platinum dissolution in aqueous acidic media under potential cycling

20 wt% Pt on Vulcan, CNF and CNT are compared. At potentials lower than 1.0 V v.s. RHE the three catalysts have very similar dissolution behaviour, with platinum concentrations below 30 ppb. This might be due to the similar properties of the finely dispersed noble metal. With increasing potential, the Pt dissolution was found increase exponentially for all the three catalysts. At 1.6 V v.s. RHE, CNF, CNT and Vulcan showed Pt concentration of 300, 421 and 1,000 ppb. Comparatively speaking, CNF and CNT supported platinum showed about 3.3 and 2.3 times less dissolution than Vulcan supported catalyst. Platinum dissolution at higher potential has been shown mainly to be due to electrochemical corrosion of carbon support[13]. In addition, based on our experience, at PEM fuel cell working temperature (≈80°C), the platinum dissolution is ten times higher than that at room temperature. The detailed experimental procedures can be found in our early publication[14].

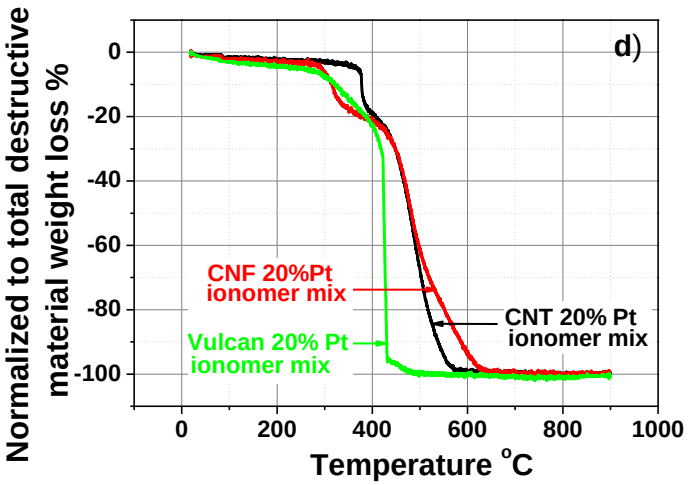

Fig. 3
An example of thermal decomposition of catalyst mixture.

Table 7 Summary for electrode electrochemical stability under cycling voltammetry treatment.

		Loading mg/cm²	Area cm²	ECSA cm²/mg	ECSA Change%	P_{Max} W_{MAx}/cm²	ΔP_{Max} %
BASF	Fresh	0.518	2.25	779	100	0.393	100
	After 5k	0.518	2.25	463	59	0.315	80
	After 10k	0.518	2.25	392	50	0.306	78
CNF	Fresh	0.529	2.25	331	100	0.195	100
	After 5k	0.529	2.25	426	129	0.276	142
	After 10k	0.529	2.25	330	100	0.218	112
CNT	Fresh	0.53	2.25	310	100	0.147	100
	After 5k	0.53	2.25	328	106	0.176	120
	After 10k	0.53	2.25	248	80	0.156	106

2.2.1.5 Catalyst single cell durability test

MEAs with identical anodes (based on Hispec 9100 catalyst, Pt/C) but different cathode Pt catalyst based on CNF, CNT and Vulcan were prepared with standard procedure, 40 wt% ionomer content. The cathode was then treated with cyclic voltammetry between 0 up to 1.6 V v.s. RHE in a single cell with hydrogen purging on the anode and nitrogen purging on the cathode. The electrochemical active surface areas of the cathode catalyst and MEA single cell performance were recorded before and after the treatment.

Electrochemical active surface area (ECSA) of the cathode in the MEA and maximum power density (P_{Max}) measured in the single cell setup before and after the cyclic voltammetry (up to 1.6 V, 5,000 cycles and another 10,000 cycles) are summarized in Table 7. Examples of the CV voltammogram polarization curves and impedance spectra for CNF are shown in Fig. 4.

Based on the evolution of the electrochemical surface areas (ECSA) as function as number of cycles between 0 and 1.4 V v.s. RHE, both CNF and CNT based cathodes showed better stability than Vulcan based. An increase of ECSA was observed in both CNF and CNT based electrodes by 29 and 6% after 5k cycles, which is probably due to an activation process or electrode structure reorganization under performance condition; however, Vulcan based electrode showed 41% decrease in ECSA after the same treatment. With a further 10k cycles, all the three electrodes showed

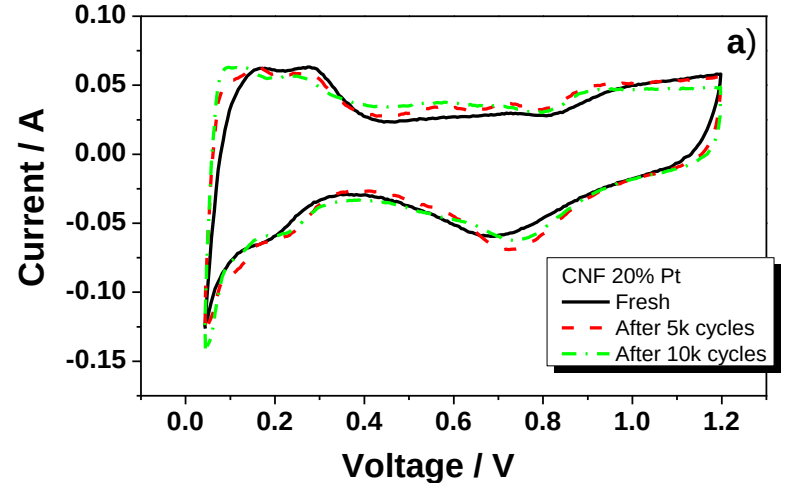

A.

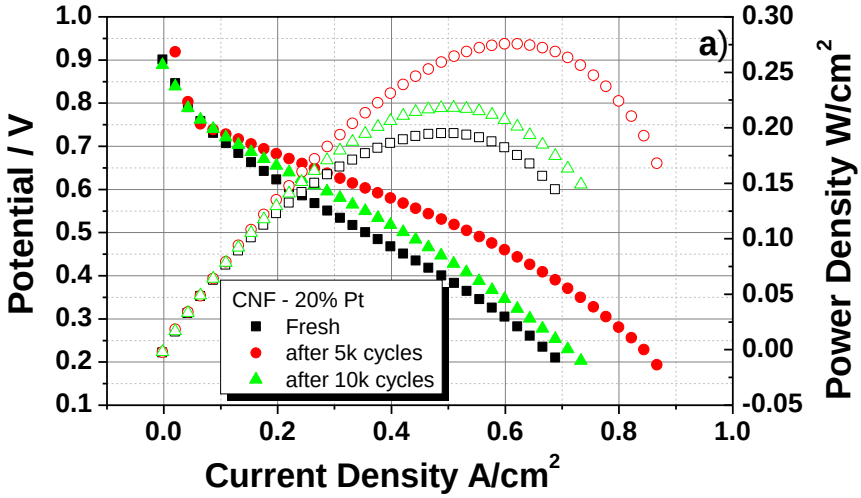

B.

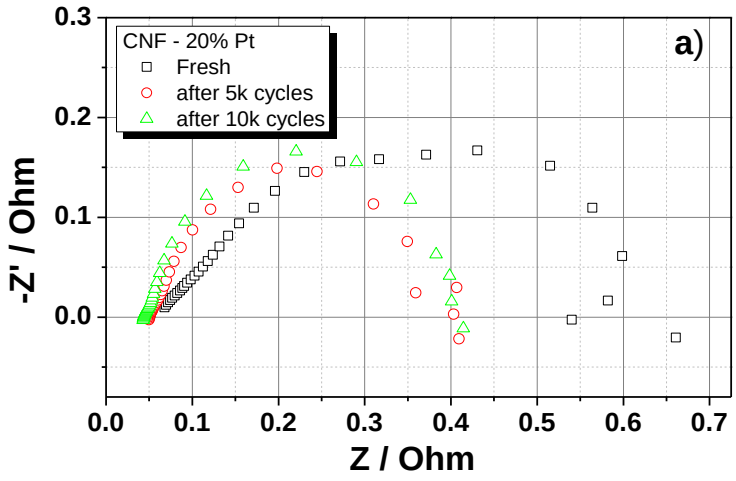

C.

Fig. 4 Example of a CV (A), a polarization curve (B) and an impedance spectrum (C) for CNF based catalyst single cell performance.

less ECSA than the starting value. This indicates that potential cycling reaching up to 1.4V v.s. RHE is harmful for the electrodes in long term.

In I-V curve, CNF and CNT based electrode showed 42 and 20% increase in max power density after 5k cycles; during the same treatment, Vulcan showed 20% decrease, which is also reflected in

the development of the ECSA. With further potential cycling, cell performances deteriorate. Similar trends were also observed in impedance spectra. In all cases, the electrolyte resistance determined from high frequency intercepts decreases, which indicates that improved electrode-electrolyte contact is part of the activation process.

2.2.1.6 Discussion and Conclusion

Carbon nanofiber (CNF) and carbon nanotube (CNT) supported platinum catalysts were prepared and optimized. The catalysts were evaluated with respect to thermal and electrochemical stability with traditional carbon black (Vulcan) based catalyst as reference. From carbon thermal stability, decomposition, electrochemical degradation in acidic aqueous media and cyclic voltage treatments, both carbon nanofiber and carbon nanotube demonstrated better stability than carbon black. High crystalline CNF showed a higher stability than CNT during the entire measurements.

In single cell testing, carbon nanofiber and nanotube based platinum catalyst did not show as good initial power density performance as the equivalent carbon black based ones, but they showed a better durability. CNF & CNT based platinum catalyst PEM fuel cells could therefore provide a more durable and more stable power source. Optimization and activation of the membrane electrode assembly – electrode structure is the key point to gain better cell performance for carbon nanomaterials.

2.2.2 CATALYST RECOVERY

Since platinum is used as the electrocatalyst in polymer electrolyte fuel cells, recovery of this expensive noble metal from discarded fuel cell membrane-electrode-assemblies is of great interest.

To dissolve and recover the platinum catalyst, the majority of available methods use hydrochloric acid leaching media assisted by a chemical oxidant such as nitric acid (i.e. *aqua* regia), halogen gas (e.g. Cl_2, Br_2), and even hydrogen peroxide[15-16]. The platinum chloro complexes thus obtained are subsequently extracted by solvent extraction processing, stripped from the organic phase by water and possibly precipitated as $(NH_4)_2PtCl_6$ in fairly high purity (99.95%) by addition of ammonium chloride to the aqueous phase[17]. Possible emissions to air from this type of processing include ammonia, chlorine, hydrogen chloride and nitrogen dioxide. The described industrial process is, seemingly, designed with the intention of recovering the noble metal catalyst as pure salts that can be traded. This line of thought is also followed in platinum catalyst recycling schemes specifically considered for polymer electrolyte membrane fuel cells[18,19,20,21&22].

Several methods exist for the preparation of supported and unsupported noble metal catalysts based on these commercially available salts[23].

The subject of the present work is an alternative approach to platinum recycling from discarded fuel cell membrane-electrode-assemblies. The idea is to bring platinum into solution electrochemically, thus avoiding the consumption of bulk chemical oxidizing agents and the associated emissions to air. Furthermore, the intention is to limit the need for purification of platinum from the acid medium by reprecipitating platinum as nanoparticles on fresh carbon substrate immediately from the acid solution with minimal pre-treatment.

A lot of knowledge on electrochemical dissolution of platinum has already been gathered through investigation of platinum dissolution as a cause of fuel cell electrode degradation (cf. section 2.2.1.4). The dissolution can lead to platinum particle growth due to re-precipitation on larger particles (electrochemical Ostwald ripening) as well as to the occurrence of platinum bands in the electrolyte membrane upon reduction of the mobile platinum ions by permeating hydrogen reactant gas.

Several electrochemical studies on pure platinum or carbon supported platinum electrodes investigate the dependence of the dissolution rate on the applied potential under static conditions and/or on the potential limits and scan rate under potentiodynamic conditions [14,24,25,26,27,28,29,30,31,32,33, 34,35&36]. An appreciable dissolution rate is found for potential cycling when the upper limit exceeds ca. +1.15 V vs. SHE, and the rate is generally enhanced when the upper potential limit is further increased[24]. Furthermore, the dissolution rate is greatly increased by the presence of chloride anions, which has been attributed to the stability of platinum chloro complexes and the hindrance of platinum surface passivation[37,38&39]. A solution of platinum chloro complexes should thus be obtainable by potential cycling of platinum in hydrochloric acid electrolyte. The choice of upper potential limit is restrained by the undesirability of chlorine gas evolution during the electrochemical process, as well as carbon corrosion, if it is desired to dissolve platinum still on its original carbon support.

The work within this project concerning the proposed electrochemical platinum catalyst recovery process, described above, is divided into the following two sections:

- Proof-of-concept of electrochemical dissolution of platinum followed by reprecipitation, from the same solution, of platinum as nanoparticles on fresh carbon substrate.
- Investigation of the applicability of the method to platinum situated in fuel cell electrode structures.

The following sections summarize the main conclusions drawn from this work. Additional information can be found in the reports enclosed as Appendices A & B. Appendix B is basically a draft for the manuscript: Nørgaard et al. (in prep): Redeposition of electrochemically dissolved platinum as nanoparticles on carbon, cf. section 6 *ibid*.

2.2.2.1 Proof-of-concept of electrochemical dissolution of platinum followed by reprecipitation

In this study, the possibility to first bring platinum into solution electrochemically and then use the resulting solution directly for redeposition of platinum nanoparticles on a carbon substrate was investigated. Pure platinum wire was dissolved by a potentiodynamic treatment in dilute hydrochloric acid electrolyte. Pure platinum was selected in order not to pollute the solution with corroded contacts or substrate, and to enable a simple gravimetric way of monitoring the amount of platinum dissolved.

The platinum containing solution was then used for redeposition with no other pretreatment than a simple pH adjustment using sodium hydroxide. Ethanol was used as the solvent and reducing agent in order to reduce the dissolved platinum to platinum nanoparticles. A commercial carbon support material was added to the reaction mixture in order to nucleate platinum directly on carbon.

The platinum-on-carbon material obtained was characterized by cyclic voltammetry, thermogravimetric analysis, powder X-ray diffraction and transmission electron microscopy (TEM) for the detection, quantification and particle size estimation of platinum. Furthermore, UV-vis spectrophotometry was carried out on the platinum containing 1 M HCl electrolyte used for the re-deposition, in order to gain insight on the form in which platinum was dissolved.

The UV-vis results showed that the potentiodynamic, electrolytic treatment led to dissolution of platinum mainly as $PtCl_6^{2-}$ ions.

As determined by thermogravimetric analysis on the product, the re-precipitation of platinum on a carbon support occurred with a high yield, meaning that virtually all the dissolved platinum was

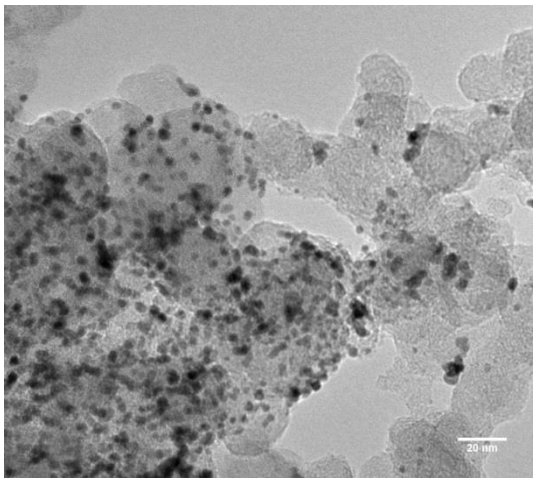

Fig. 5
Transmission electron micrograph of platinum redeposited as nanoparticles on carbon support. Prior to redeposition, the platinum was dissolved electrochemically.

converted into metallic platinum on carbon support. The aforementioned pH adjustment of the solution prior to rep-recipitation proved necessary for the high yield when platinum was dissolved in 1 M HCl electrolyte.

In addition to the gravimetric determination, the successful precipitation of platinum on carbon was verified by the clear platinum features observed in cyclic voltammetry, the occurrence of peaks characteristic of platinum in the X-ray diffraction pattern, as well as by the electron micrographs obtained by TEM (Fig. 5).

The platinum particle size was consistently found to be in the range of 4-5 nm using three different methods: TEM imaging; crystallite size estimation by application of the Debye-Scherrer equation on the X-ray diffraction data; and finally, the particle size estimate obtained via the platinum surface-area-to-mass ratio and the assumption of perfectly spherical particles (where the surface area is determined from cyclic voltammograms recorded in argon saturated electrolyte, and the mass is determined by the thermogravimetric analysis).

Thus, platinum metal can be dissolved electrochemically and subsequently re-deposited as nanoparticles on a carbon substrate, without intermediary separation and handling of pure platinum salt. This enables circumvention of the emissions of ammonia, chlorine, hydrogen chloride and nitrogen dioxide associated with conventional processes for recycling of platinum catalyst from polymer electrolyte fuel cell electrodes.

2.2.2.2 Applicability of the method to platinum situated in fuel cell electrode structures

The work described in section 2.2.2.1 use pure platinum wire as the source of platinum, and granted does not answer all questions which must be answered before the concept of electrochemical dissolution with subsequent re-deposition of platinum can be applied as a method for recycling platinum catalyst from fuel cell MEAs.

For one thing, the concept requires proper electrical contact to the platinum particles throughout the dissolution process. In relation to direct electrolysis on MEAs, this contact may have been compromised through degradation during the lifetime of the MEA under fuel cell operating conditions. This will interrupt the electrical connectivity and thus render part of the platinum inaccessible for electrolysis.

Experiments with fresh (= unused) electrode layers showed that virtually all platinum could be brought into solution and thus recovered from the electrode by potential cycling in 1 M hydrochloric acid electrolyte. This indicates that platinum and the carbon support constitutes a continuous electrically conductive phase at the beginning of life for the fuel cell electrodes.

However, potential cycling experiments in 1 M hydrochloric acid on a used MEA, run for 2,884 hours in a fuel cell, in combination with experiments on electrochemically aged electrode layers revealed that as the platinum catalyst degrades during fuel cell operation, some of the platinum, though still in the electrode, loses electrical contact to the carbon substrate. Therefore, the yield of platinum recovery by electrochemical means will decrease as the extent of catalyst degradation increases during fuel cell operation; unless actions are taken that ensure the electrical connectivity.

One approach to this problem, which may be considered, is to first separate the platinum from its co-constituents (carbon and ionomer), and subsequently dissolve the platinum by electrolysis in an electrochemical fluidized bed setup. This and other means to ensure the sustainment of electrical contact to the platinum particles during electrolysis are among the subjects within the DuRaPEM III project.

2.3 MEMBRANE

2.3.1 CATION EXCHANGE SELECTIVITY OF PERFLUORINATED SULFONIC ACID MEMBRANE

Formation of sulfonic anhydride S-O-S (from condensation of sulfonic acids) is known as a possible degradation mechanism for Nafion® membranes under hydrothermal aging condition[40], which is especially critical for hydrogen fuel cells. A similar mechanism may also contribute to the membrane degradation in direct methanol fuel cells (DMFCs), where liquid water has direct contact with the electrolyte. Therefore an equivalent condition in aqueous environment (swelling-dehydration cycle) was established to test the degradation mechanism in Nafion membrane for better understanding of DMFC degradation[v].

2.3.1.1 Major observant and result

- Physical change of the membrane

After more than 60 swelling-dehydration cycle, almost 15% of the membrane hydrated weight was lost. This is in a clear contrast to the membrane dry weight, which is seen rising with the number of cycles up to 2.6%, as shown in Fig. 6.

The membrane thickness in both hydrated and dried state follows an exponential decay with the cycles. The thickness was reduced by 15% (hydrated) and 12% (dried) at the end of the test.

- Membrane resistance and attached water

At the end of the test, the resistance of the membrane is more than 15 times higher than for the original state; the attached water per sulfonic group drop from 24 to 15.

- X-ray Photoemission Spectroscopy

[v] These results are compiled in a peer-reviewed paper (Appendix C: "Cation exchange selectivity of perfluorinated sulfonic acid membrane"). Major observation and conclusion is mentioned in this report; detailed experimental description can be found in the paper.

Based on XPS analysis, there is a clear trend that the relative amount of fluorine decrease and oxygen increase with increasing number of cycles. For carbon, a slight rise at the early stage was observed after which a constant was reached. This suggests fluorine release during the cycles, and most likely from the carbon – fluorine back bone. This is also supported by the relative increase of the oxygen content in the membrane. The detection of silicon was unexpected; however, the systematic appearance of Si indicates a surface contamination during the cycle treatments.

- Fluoride release

A fluoride concentration of 10^{-5} mol/L was then detected in the adsorpted water after over 60 cycles of swelling – dehydration.

- IEC and re-activation

Almost100% proton ion exchange capacity was lost after the 64 cycles. However, complete IEC was regained after the membrane was boiled in 1M sulphuric acid for one hour. Also the other properties of Nafion were recovered.

- SEM, EDX and Raman spectroscopy

As suggested by the EDX element analysis and Raman spectroscopy, during the treatment, Nafion was contaminated with calcium.

2.3.1.2 Discussions

- Formation of sulphur anhydrate

Formation of sulfonic anhydrate is a well-established degradation mechanism for Nafion at elevated temperature and changing humidity. The reaction mechanism is displayed below

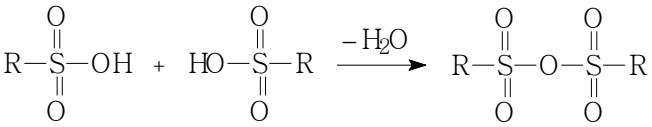

Due to the formation of sulfonic anhydrate, decrease in water content, ion exchange capacity, conductivity etc. are observed. The most direct detection of the anhydrate formation was demonstrated using infrared spectroscopy: a foreign peak at 1440 cm^{-1} corresponding to SOS bonding evolved.

In order to distinguish the difference between two possible degradation mechanisms for Nafion operated with liquid water as in Direct Methanol Fuel Cells (DMFCs) and Nafion operated with water vapour as in PEMFC, Nafion samples was also treated at 80ºC, 80% RH for comparison with the water boiled samples. For original, Ca ion exchanged and water boiled sample after 62 cycles, hardly any SOS bonding was detected. While for 80ºC, 80% RH treated Nafion, a clear sulfonic anhydrate was observed by IR, as reported by many other groups as well. This suggests that there are different dominating degradation mechanisms possible for the two types of polymer membrane fuel cells (DMFC and PEMFC).

- Stability of sulphur anhydrate

S-O-S bonding is proven to be stable within water and boiling water but dissociates in acid and ionic environments. This indicates that the sulfonic group has a higher affinity to ions rather than to

Table 8 Examples from the literature of accelerated test protocols for evaluation of mechanical membrane durability.

Relative humidity	T	Detection of perforation	Ref.
30-80% RH and 80-120% RH (condensing) in humidity chamber. 30 min.s per cycle	65ºC	Post treatment SEM as well as mechanical analysis	41
0-100% RH by switching between dry and humidified streams, 10 minutes dry, 40 minutes humid	70ºC	H_2 crossover current measured by linear sweep voltammetry, as well as infrared imaging	42
0-150% RH by switching every two minutes between dry and supersaturated streams	80ºC	Measurement of air permeation upon application of differential pressure	46,43&44
0-100% RH by switching between dry and humidified streams every hour	100ºC	Measurement of air permeation upon application of differential pressure	45

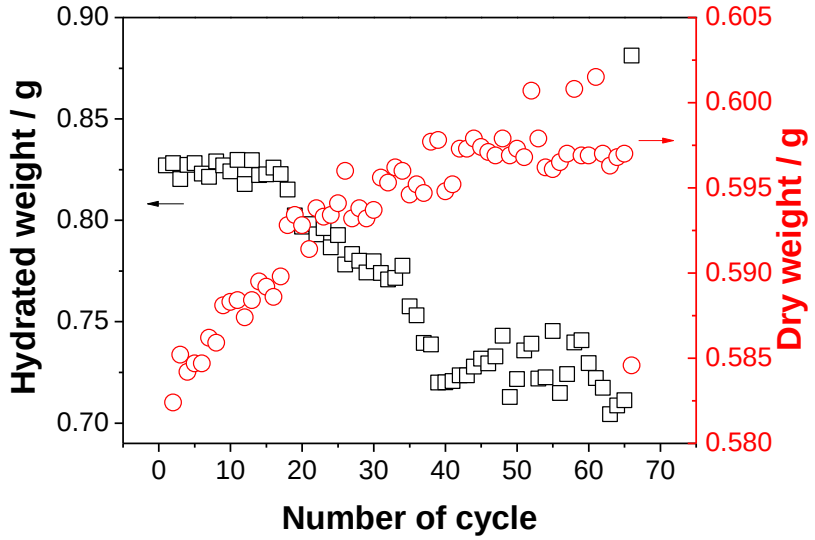

Fig. 6
Weight change for hydrated and dried form. (The last point is after acid activation).

the formation of anhydrate. This implies that formation of sulfonic anhydrate is unlikely when free ion is accessible. Similar observation was also detected for the sample treated at 80ºC 0%RH.

- Sulfonic acid group affinity test

It is shown that iron has a higher affinity towards sulfonic acid group compared to calcium, which in turn has a higher affinity than sodium. This is to be expected as the surface charge density on the ion increase with the ionic charge.

There is also a clear trend showing that higher the valence of the cation, higher resistance of the product membrane. This is probably due to the fact that more complex ionic network impedes membrane hydration and consequently lower content of water and sluggish movement of protons.

2.3.1.3 Summary

For oven baked virgin Nafion (80ºC, 80% RH), a clear peak showing S-O-S bonding was found, which was not observed in swelling – dehydration cycled samples. This may be due to both the difficulty of water condensation in liquid environment, and more likely, to a strong affinity between $-SO_3^-$ and miner amount of free ions. This suggests that instead of sulfonic anhydride formation,

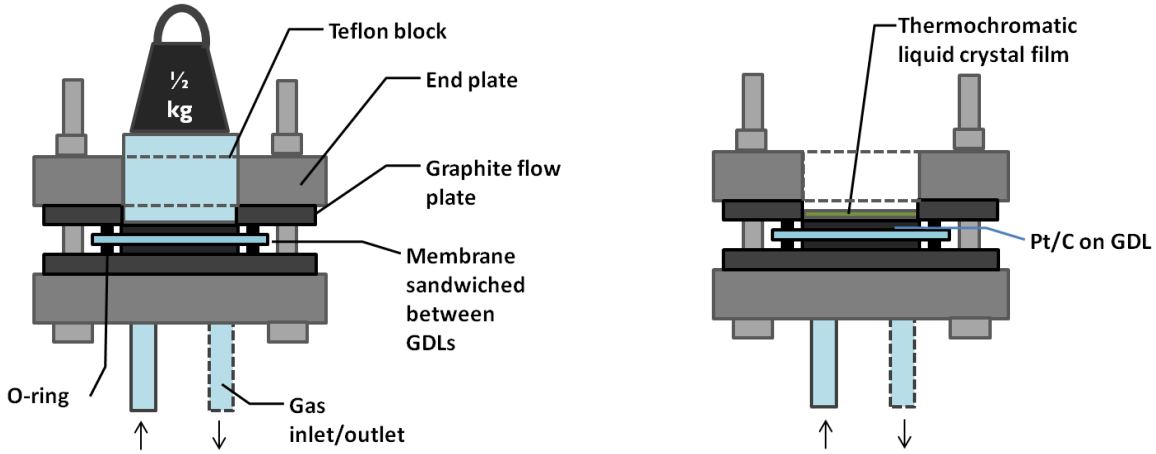

Fig. 7 Configuration of the cell assembly during relative humidity cycling (left) as well as during thermal mapping (right). The relative humidity was cycled between 30 and 80% RH at 65ºC but also between 40 and 90% RH at 60ºC. In both cases, the air was forced to circulate using a pump. For thermal mapping, 7% hydrogen in argon was supplied to the gas inlet at room temperature.

cation contamination is a more important membrane degradation mechanism in a cell where Nafion is exposed to a liquid phase, such as in a DMFC.

Major changes observed in Nafion after more than 60 times swelling – dehydration cycles include decreasing water content, decreasing thickness, decreasing surface fluoride, increasing resistance, increasing dry weight and a changed surface morphology. Sulfonic acid groups in Nafion was found having a high affinity towards high valence cations (e.g. Fe^{3+} and Ca^{2+}) comparing to low valence ones (e.g. Na^{+}). During operation of DMFC fuel cells, high valence cation contaminations can be fairly easily introduced in the membrane system (through e.g. air circulation, or water cooling system) and may cause reduced performance. Fortunately the effect is reversible in the sense that the original properties may be restored by an acid wash. Irreversible degradation as indicated by fluoride release was found to be insignificant.

2.3.2 Membrane mechanical durability during relative humidity cycling

The presented work within this section is performed as a joint effort between the present project and the MAProCon-project (DSF grant no. 2104-08-0016, project acronym).

Means of assessing the susceptibility towards and spatial origin of pinholes in fuel cell membranes were pursued. For this purpose the accelerated test protocol should focus on mechanical failure modes and exclude influence from chemical degradation. The in-plane compressive and tensile stresses associated with dimensional changes upon swelling and dehydrating the membrane when constrained in the fuel cell is considered the biggest thread to long-term mechanical durability[46]. Repeated cycling between humid and dry conditions creates fatigue, which can lead to membrane fractures, whereas the viscoelastic creep exhibited by the stressed membrane can lead to pinhole formation due to local thinning. Examples of protocols, found in the literature, for examining the resilience of constrained membranes under cycles in relative humidity at constant temperature by periodically checking for membrane perforation are listed in Table 8.

An approach resembling the first entry of Table 8 was applied primarily due to the fact that a humidity chamber (Memmert HCP 108) was available in our lab, whereas a system for frequent, rapid gas switching was not. The appeal of using infrared imaging and the exothermic reaction

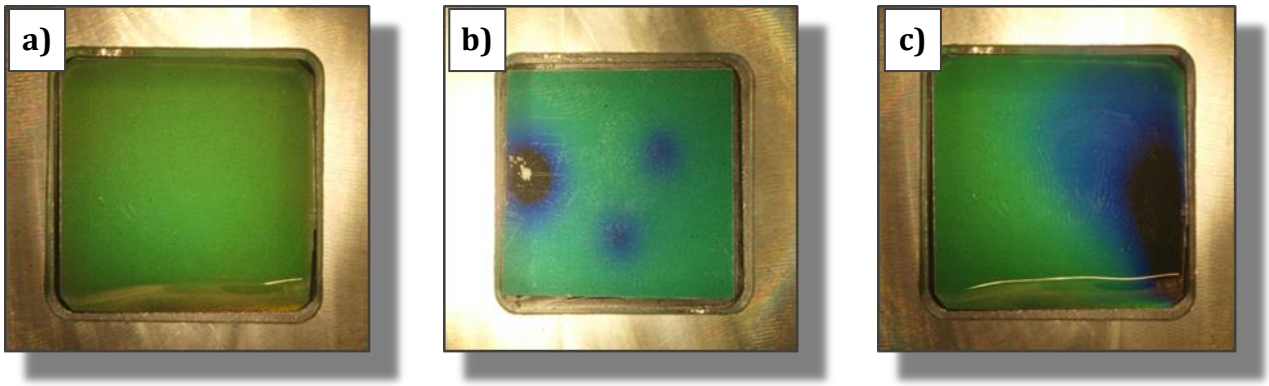

Fig. 8 Top view pictures of thermal mapping using thermochromic film: a) Nafion 117 reference picture (without hydrogen flow); b) Nafion 117 deliberately perforated using a needle; c) Used MEA with pinholes, supplied by IRD Fuel Cells.

between permeating hydrogen and oxygen to map the position of any membrane perforations formed was also considered. The cost of infrared imaging equipment with the necessary resolution put an end to that endeavour. However, a cheaper method for thermal mapping using thermochromic liquid crystal films was pursued instead.

The chosen setup is depicted in Fig. 7. The membrane sample was mounted in a single cell design (supplied by IRD Fuel Cells A/S) open to one side in order to enable thermal mapping. During cycling, the membrane was constrained by stacking a carbon gas diffusion layer complete with porous carbon catalyst support, a Teflon block, as well as a 0.5 kg weight (in that order) on top of the horizontally arranged membrane. The cycling was done between 30 and 80% RH at 65ºC and also at 40-90% RH at 60ºC. The relative humidity and temperature conditions were chosen as a compromise between mutually excluding requests: As high a temperature and as large a relative humidity span as possible combined with a minimal cycle time and avoidance of condensation in the chamber. As the chamber uses intake of ambient air for drying, very low relative humidities were not an option.

The membrane and gas diffusion layers (GDLs) were not hot-pressed together. Thus, it was possible to swap the upper GDL for a GDL with carbon supported platinum catalyst on one side and a thermochromic liquid crystal film adhered to the backside of the GDL. The liquid crystal film was supplied by Edmund Optics (#83-908, 20–25ºC temperature range). The platinum catalyst was used to catalyse the reaction between permeating H_2 (7% in Ar) and O_2 (air) used for thermal mapping.

2.3.2.1 Results

Fig. 8 exhibits pictures illustrating the utility of the thermochromic film used for thermal mapping in relation to the test of membrane mechanical durability by relative humidity cycling. The Fig.s shows how a clear contrast was achieved on the film when a deliberately perforated Nafion 117 membrane as well as a used membrane-electrode-assembly, known to have pinholes, were thermally mapped. Despite the apparent utility of the thermochromic film, the results of relative humidity cycling for investigation of mechanical durability of the membranes did not become as bountiful as hoped. Even after 2,000 relative humidity cycles (>80 days), no pictures distinguishable from Fig. 8a were obtained, indicating that the test conditions chosen did not results in severe enough degradation for pinholes to be detected by this method.

2.3.2.2 Discussion and conclusion

It appears the applied conditions are not severe enough to achieve a sufficiently accelerated mechanical degradation test. It is not feasible to accelerate the test further using the humidity

chamber at hand, since increasing the upper relative humidity limit will risk condensation issues whereas decreasing the lower limit is not an option without introducing drying of the air taken in by the chamber. Instead, the use of dry gas/air in conjunction with a by-passable humidifier is recommended in order to enable fast switching between 0% and 100% relative humidity, for instance by using solenoid three-way valves.

2.4 AST MEMBRANE TESTS

Sudden death of LT PEMFC MEAs occurs. This quickly EoL is most often related to development of membrane pin-holes. It has therefore been important to perform ex-situ membrane tests to screen commercial available membranes and perform further tests with the most promising membranes. Several LT PEM membranes have therefore been tested using the DOE AST-protocol on 'MEA Chemical Stability and Metrics'[47], the results is shown in Fig. 9. The test is defined for 200 hours, EoL is defined when the hydrogen crossover rate exceeds 30 mA/cm^2. There is only one of the tested membranes that successfully pass the test (Reinforced Nafion). These results have made IRD to change the membrane to Nafion XL (reinforced Nafion) in their standard MEAs. This has had a big impact on the MEA durability and lifetime.

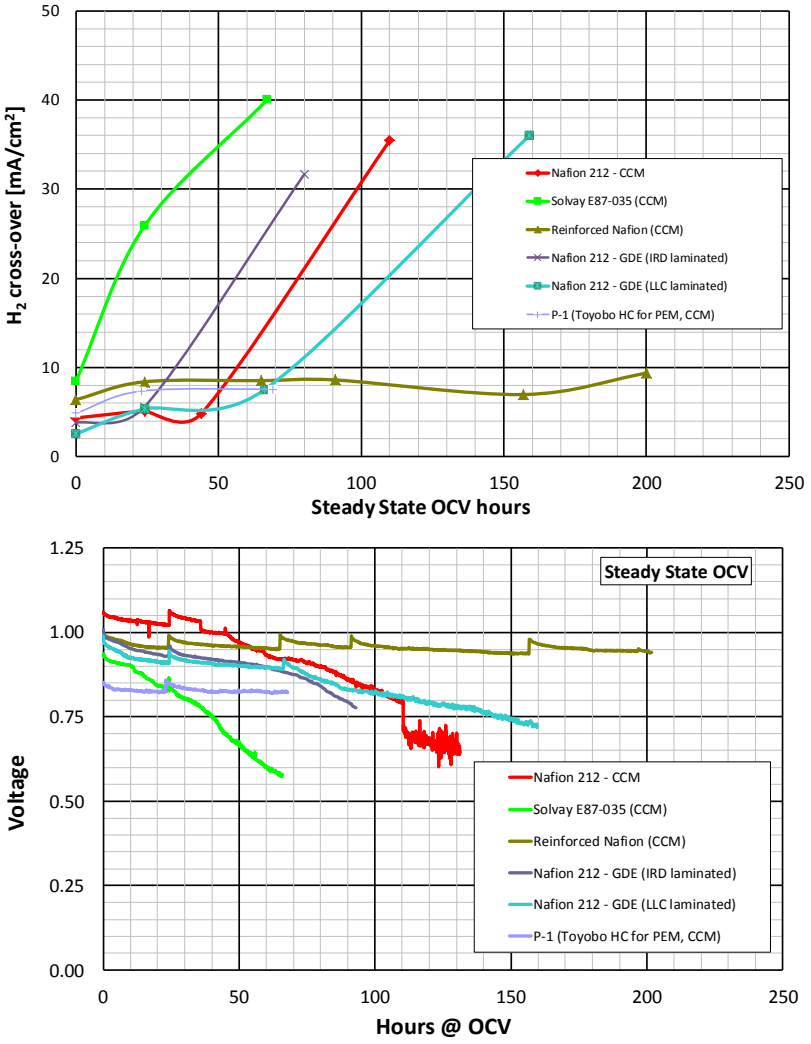

Fig. 9 LT PEMFC membrane ex-situ tests. A) Development of hydrogen crossover; and B) The development of OCV during the ex-situ test.

3. LT PEM

3.1 Introduction

The performance of a PEM fuel cell or stack is affected by many internal and external factors, such as fuel cell design and assembly, degradation of materials, operational conditions, and impurities or contaminants. Performance degradation is unavoidable, but the degradation rate can be minimised through a comprehensive understanding of degradation and failure mechanisms. It is relevant to define the following terms in order to clearly understand the concepts of PEM fuel cell lifetime and performance decay discussed in following sections:

- *Reliability*: The ability of a fuel cell or stack to perform the required function under stated conditions for a period of time. It includes failure modes that can lead to catastrophic failure and performance below an acceptable level.
- *Durability*: The ability of a PEM fuel cell or stack to resist permanent change (irreversible) in performance over time. Durability decay does not lead to catastrophic failure but simply to a decrease in performance that is not recoverable or reversible (i.e., due to loss of electrochemical surface area, carbon corrosion, etc.). This issue is related to ageing.
- *Stability*: The ability to recover power lost (reversible loss) during continuous operation. Stability decay is always concerned with operating conditions (such as water management) and reversible material changes.

3.2 LT PEM Single Cell Tests

Two (2) types of MEAs have been tested (Table 9). One set of MEAs are equipped with ordinary IRD Pt/Ru anodes that are capable of reformate operation, the other set of tested MEAs are equipped with pure Pt-anodes. The purpose was to investigate the Ru-alloy catalyst stability on the anode. All the other MEA precursors are identical for all five (5) MEAs. The MEAs have been exposed to two different load densities (Table 9).

The single cell durability testing is done on 50 cm^2 cells. The cells are operated at constant load for 250 hours and then characterised electrochemically (IV, H_2 crossover, ECSA etc.). It is important to bear in mind that the challenge of water management is not addressed in a quantified manner within the present study.

Table 9 Summary of the single LT PEM MEA test results.

MEA	Anode [mg/cm²]		I	BoL U_{Cell}	Test hours	Degradation		Comments
	PtRu	Pt	A/cm²	mV		Steady state µV/h	IV/LSQ µV/h	
1645	0.3	-	0.33	730	6,135	-17	-11	
1647	-	0.2	0.33	753	6,086	-38	-22	Was air starved after 2,500 test hours
1646	0.3	-	0.65	586	10,025	-11	-0.6	
1648	-	0.2	0.65	627	1,517	-133	-	
1732	-	0.2	0.65	440	3,194	-32	-	OCV several times for longer periods of time

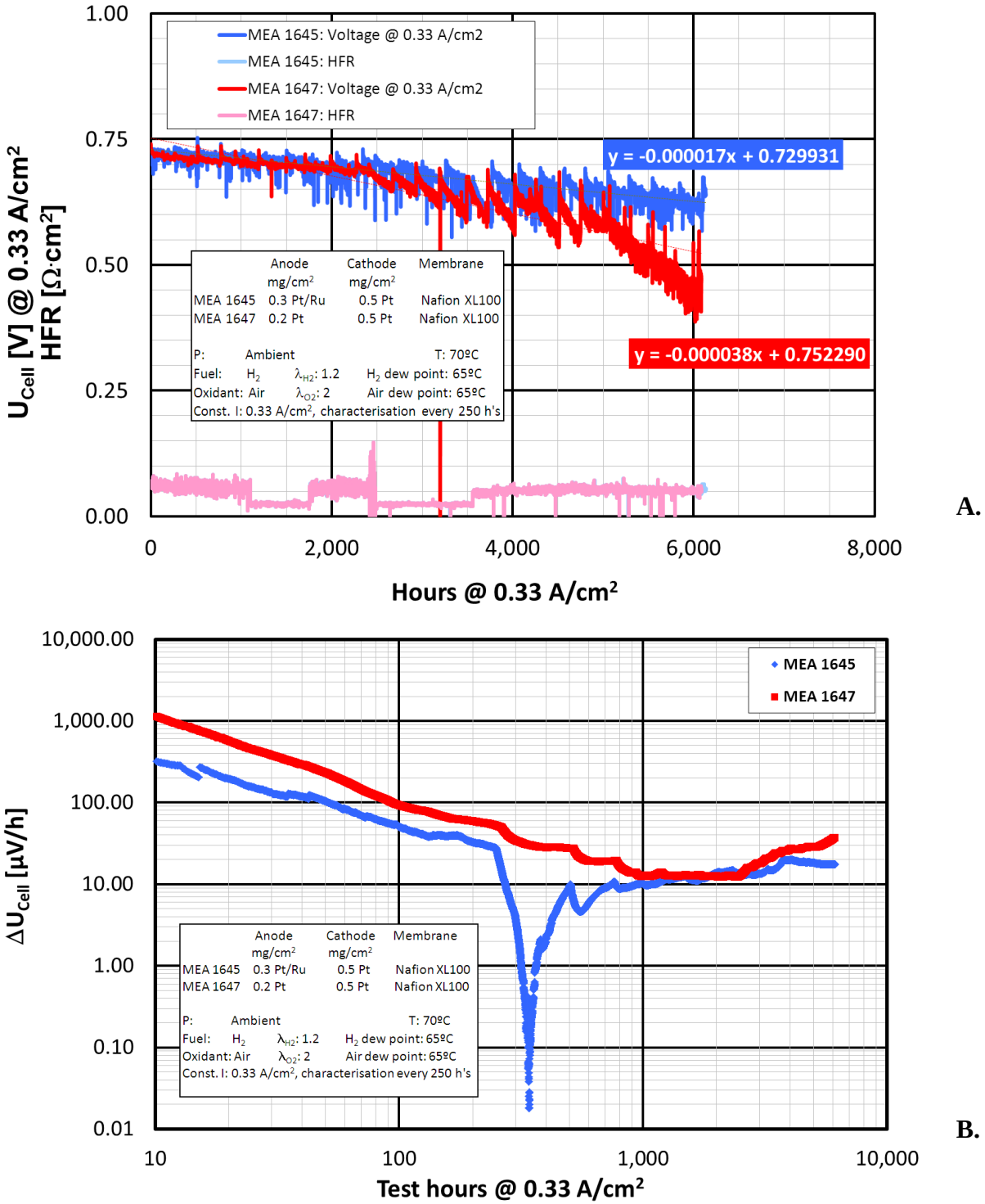

Fig. 10 Performance (A) and degradation rate (B) of MEA 1645 & MEA 1647.

The results for the two (2) MEAs loaded continuously at 0.33 A/cm^2 are shown in Fig. 10. The two MEAs perform equally the first 2,500 hours (Fig. 10A). MEA 1647 was unfortunately air starved at this time, which permanently damaged the MEA. This is very pronounced in the degradation rate that increases constantly after this incident (Fig. 10B). It is obvious from this type of data that the decay rate is not constant; the degradation is decreasing with time, and for the MEA 1645 with

PtRu-anode it is significantly affected by the characterisation every 250 hours although this effect is not permanent.

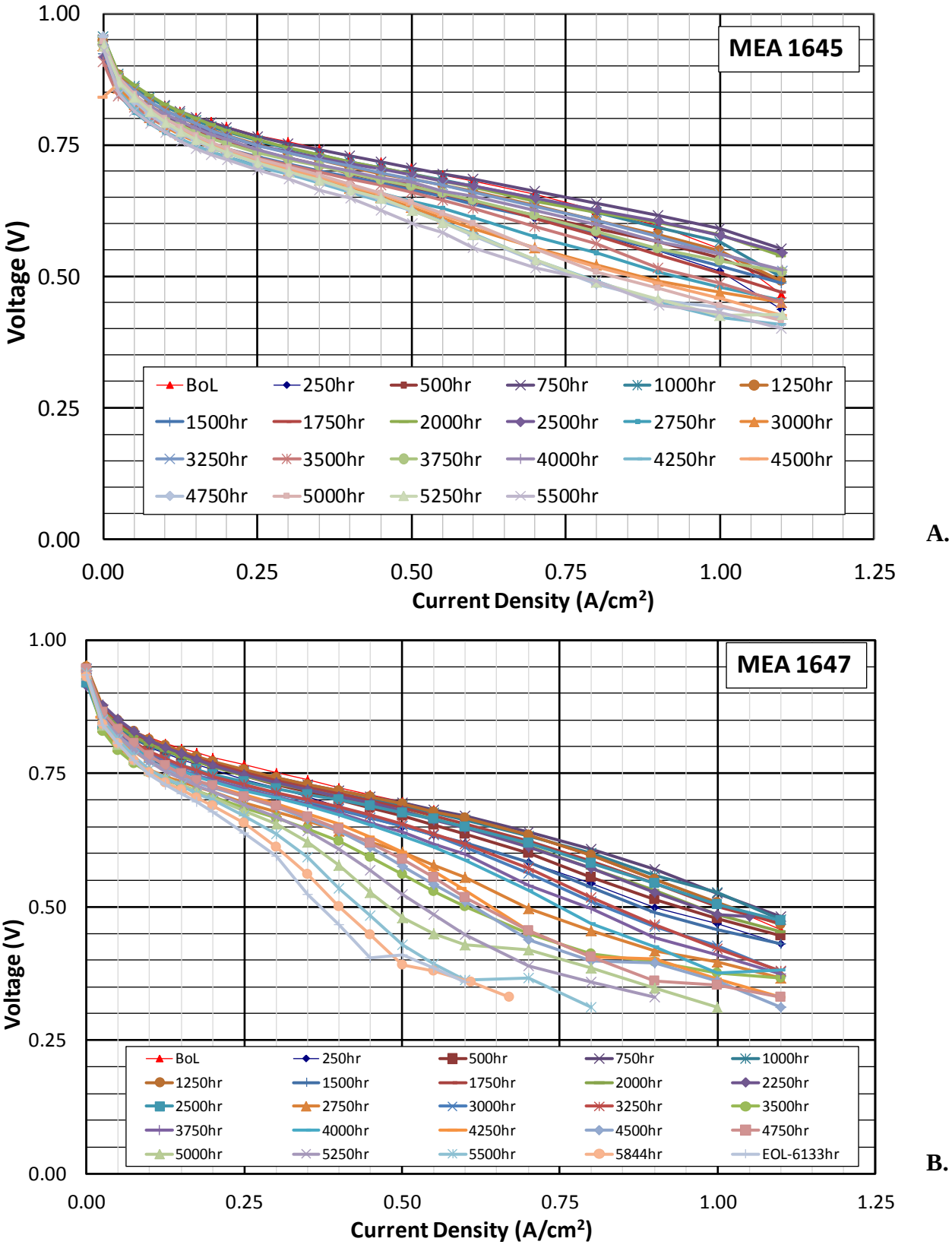

Fig. 11 Performance characteristics of MEA 1645 (A) & MEA 1647 (B), respectively.

The I-V characterisation of MEA 1645 & MEA 1647 is shown in Fig. 11. A LSQ-fit has been calculated for each I-V curve. The LSQ results have been used to calculate the MEA durability (Fig. 12) that are markedly lower than the MEA stability at steady state (Fig. 10). The two MEAs (1645 & 1647) have also been characterised with respect to development of membrane failure and electrochemical active surface area (Fig. 13). The results show no crossover development (Fig. 13A) and a significant loss of cathode ECSA, hence a reduction of 50% ECSA occurs over the first 2,000 hours of operation.

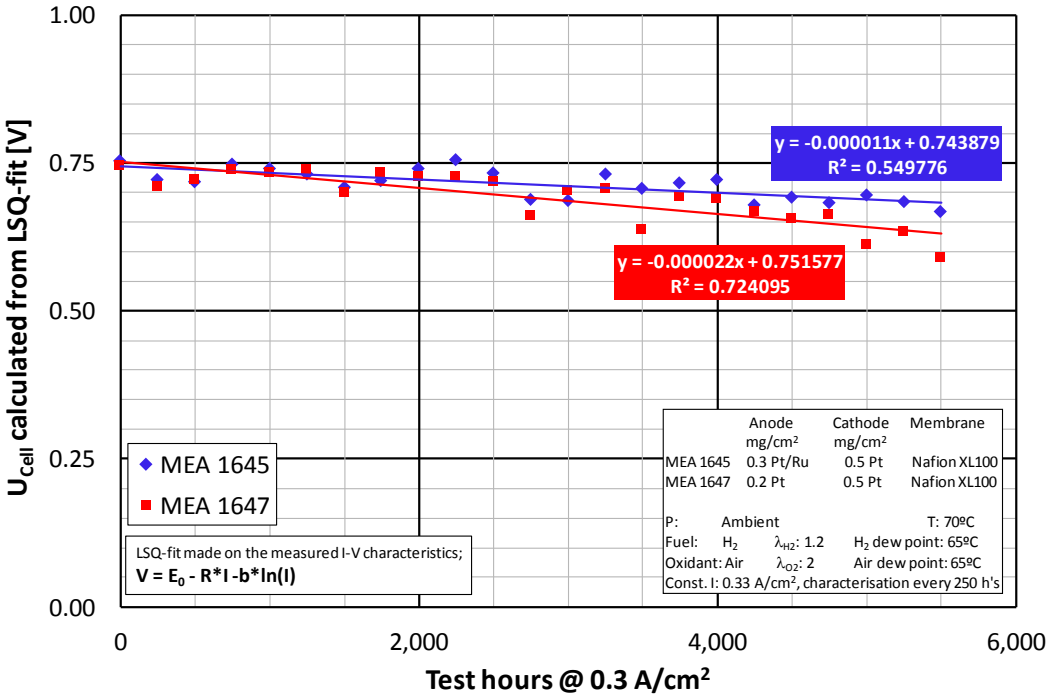

Fig. 12 The calculated performance at 0.33 A/cm^2 using the LSQ-curve fitting results for MEA 1645 & MEA 1647.

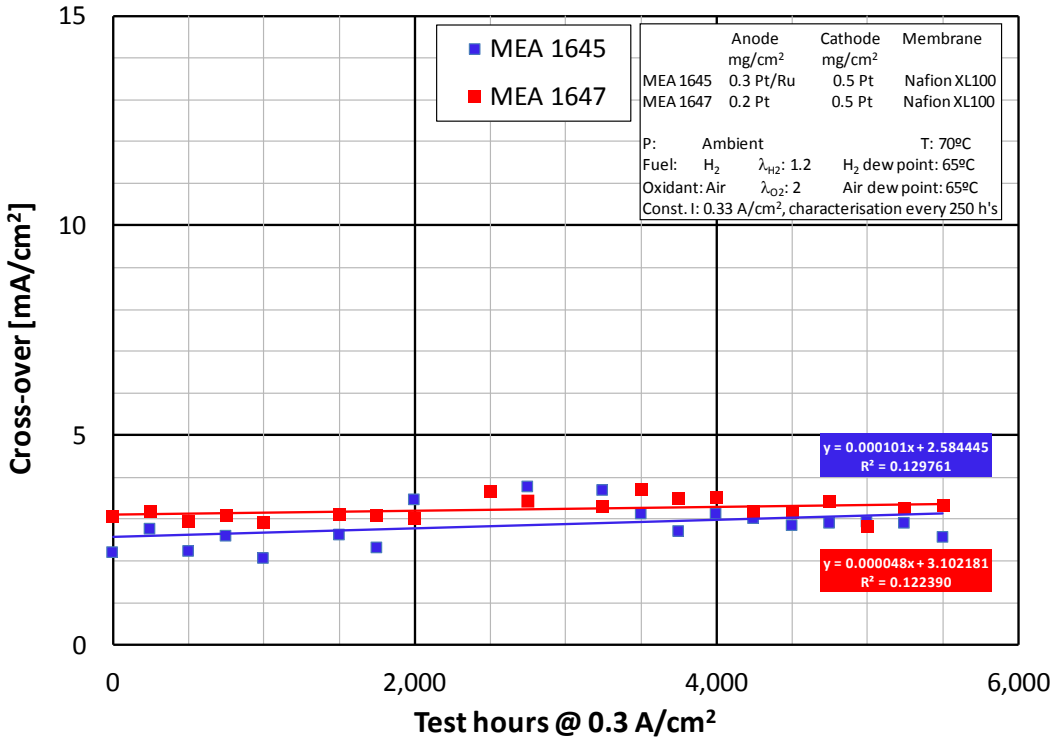

A.

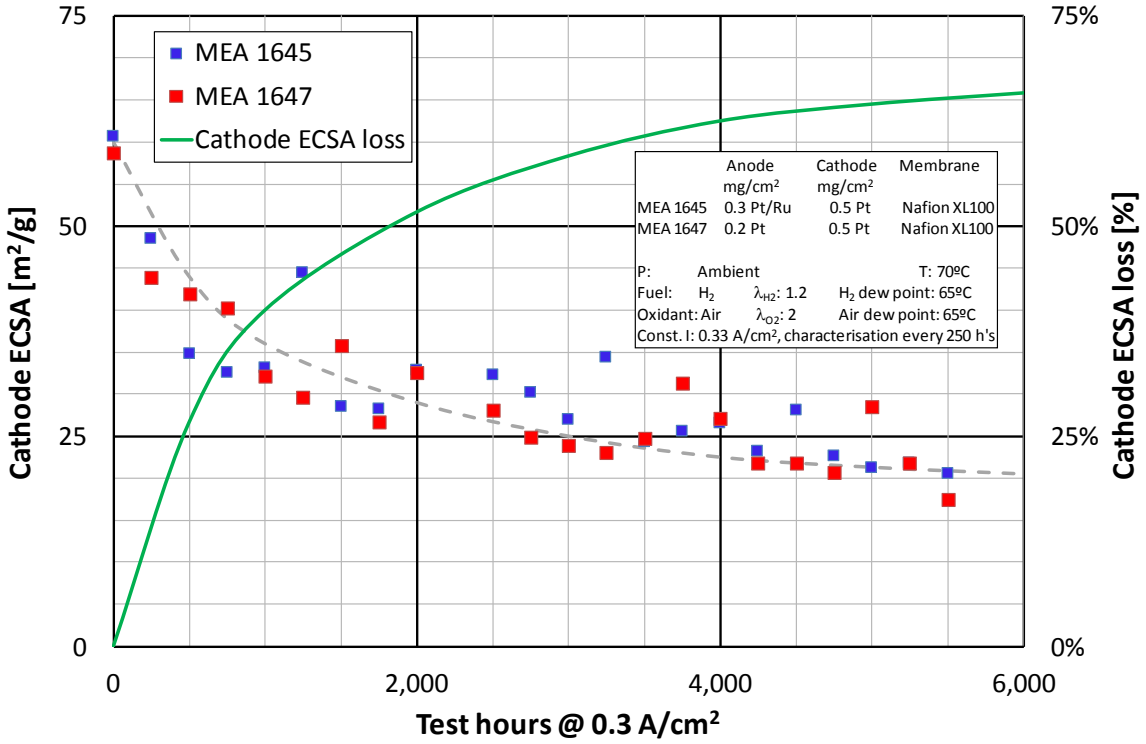

B.

Fig. 13 Results of the MEA 1645 & MEA 1647 characterisation.

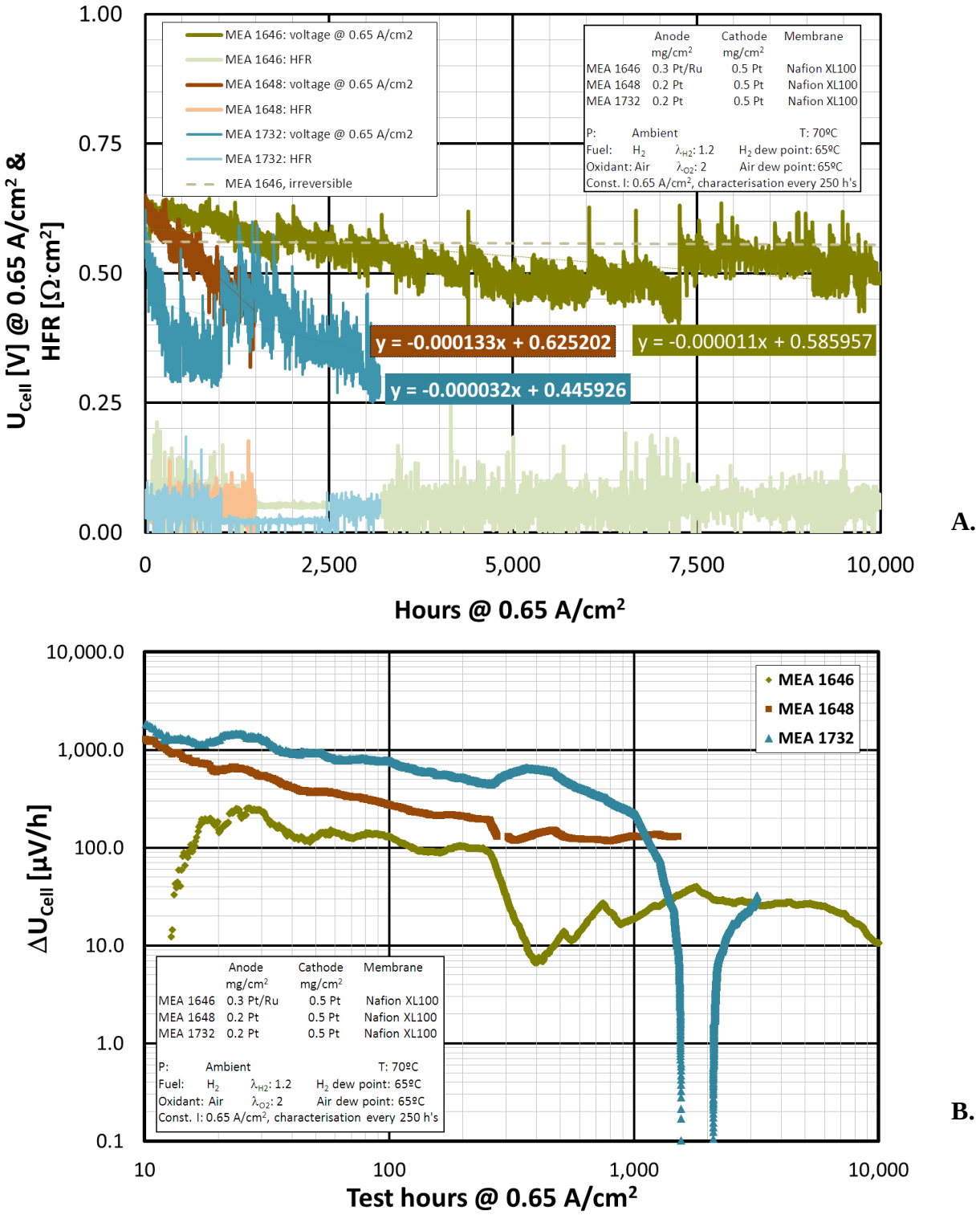

Fig. 14 Performance (A) and degradation rate (B) of MEA 1646, MEA 1648 & MEA 1732.

The results of the MEAs tested in steady state at 0.65 A/cm^2 are shown in Fig.s 14-17. Experimental difficulties occurred during test of both MEA 1648 and MEA 1732. The results from both these two MEAs are therefore disregarded in the following.

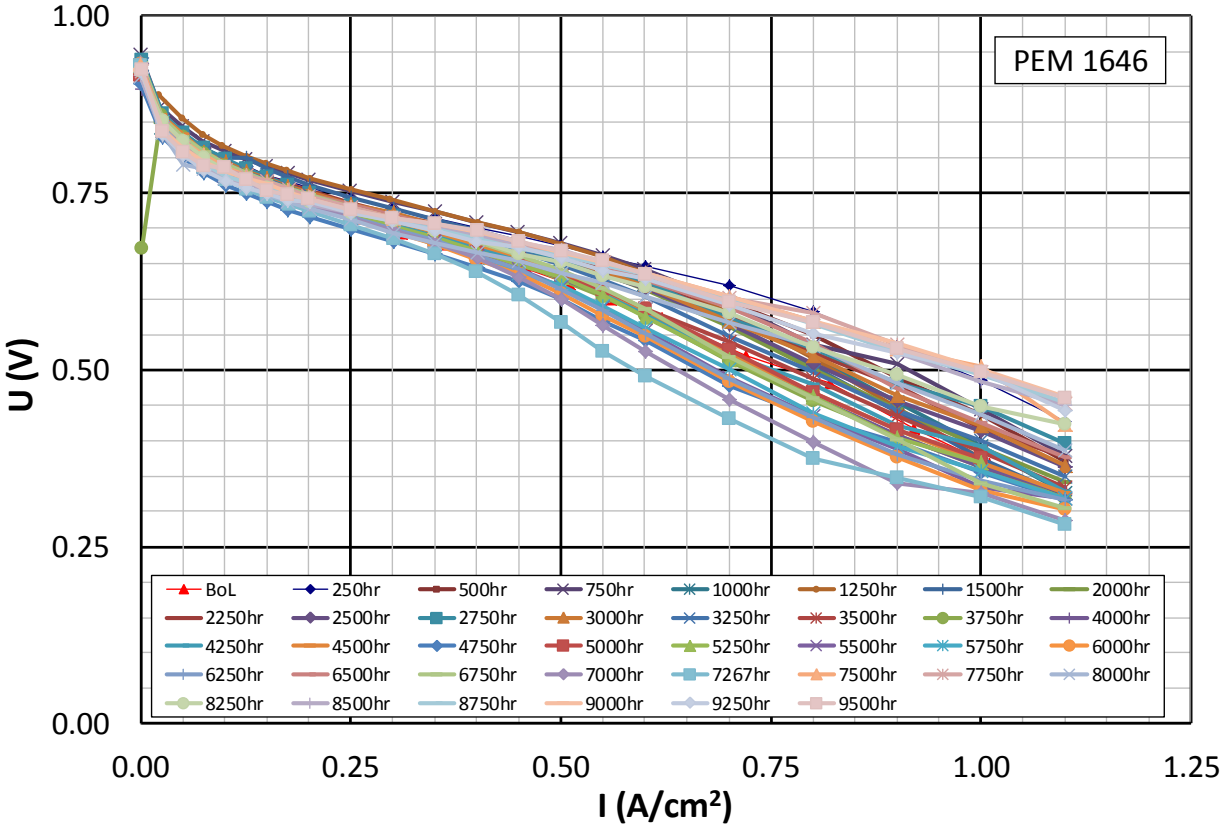

Fig. 15 Performance characteristics of MEA 1646.

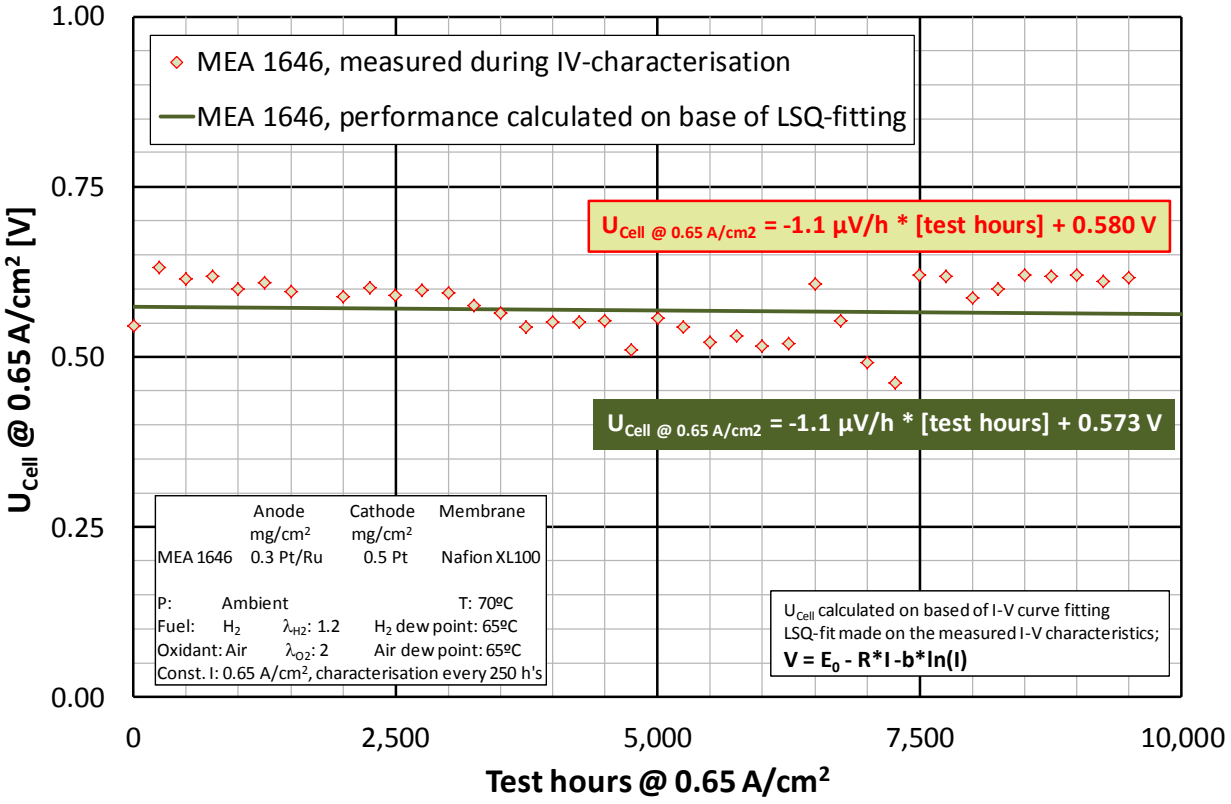

Fig. 16 The measured performance (Fig. 15) and the calculated performance based on LSQ-fit of the I-V characterisations at 0.65 A/cm^2 for MEA 1646.

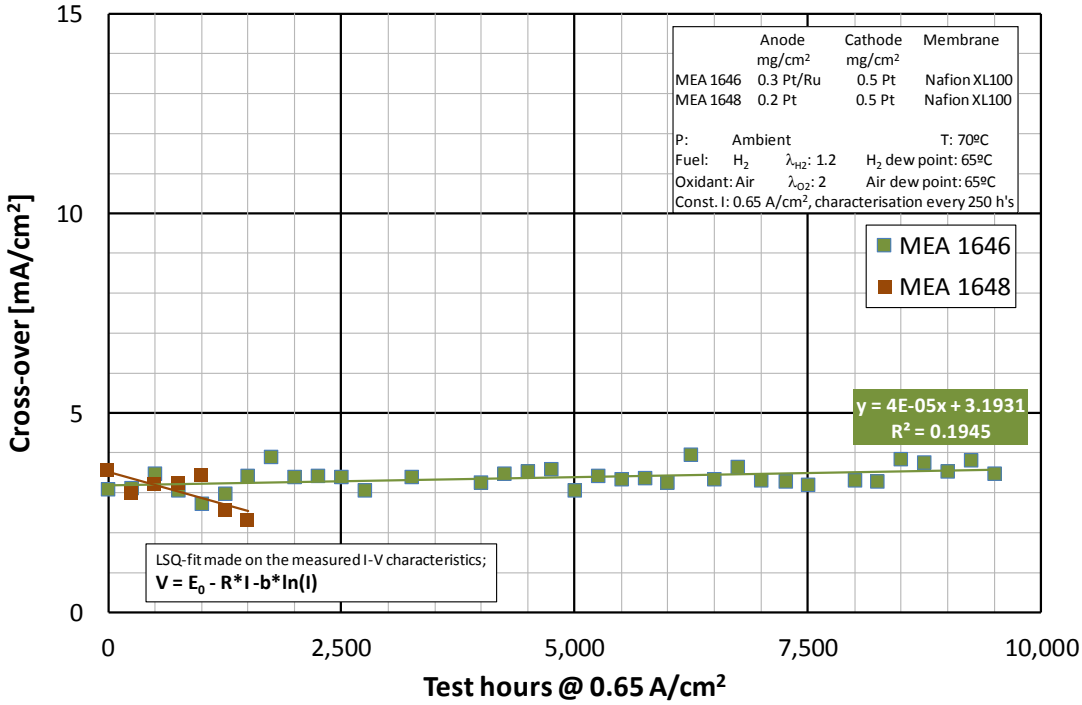

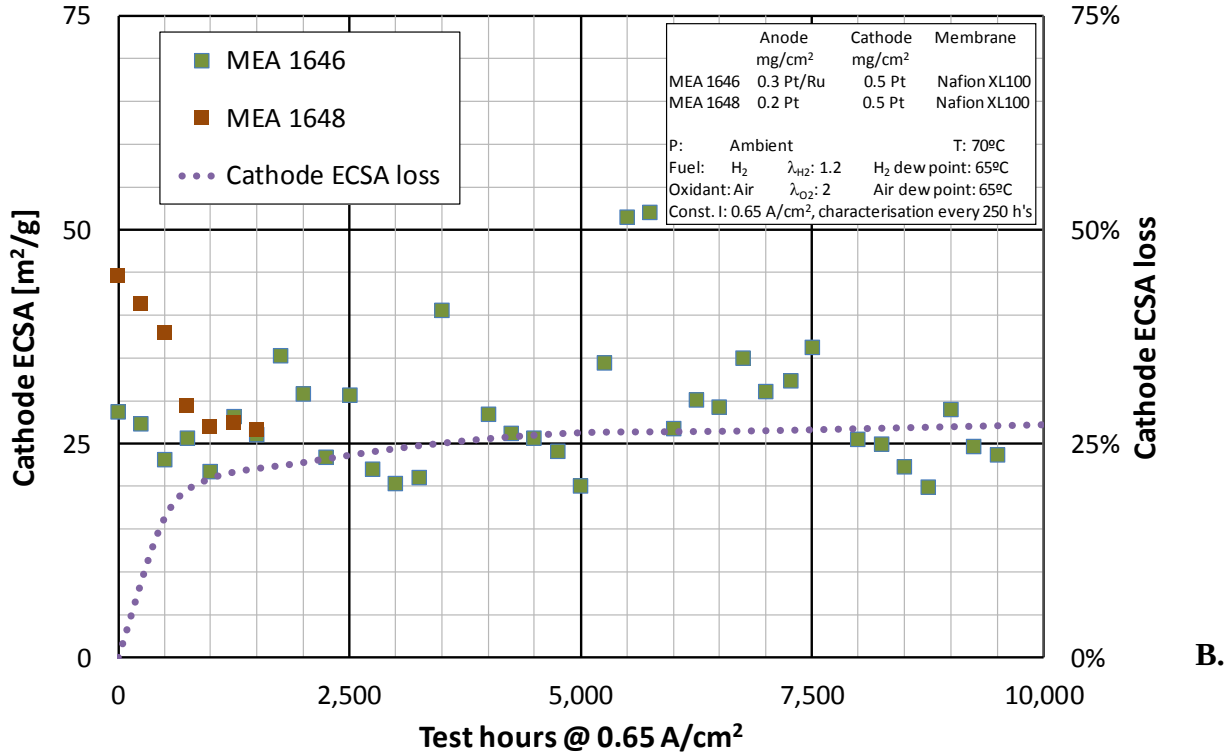

Fig. 17 Results of the MEA 1646 (& MEA 1648) characterisation.

The results for MEA 1646 confirm the conclusions made for the MEAs loaded at 0.33 A/cm^2 discussed previously. Some results for the MEA 1646 are even more pronounced than noted for the other MEAs. MEA 1646 has been tested for more than 10,000 hours. The degradation calculated from the steady state operation is 11 µV/h (Fig. 14), while the degradation calculated from the I-V characterisation only is 1 µV/h. It can be concluded that only a small fraction of the degradation measured at steady state is irreversible, as the degradation observed in the I-V characteristics is

more likely to represent the irreversible degradation. There might be more than one explanation for the decay observed in steady state operation, e.g. electrode & GDL flooding that is removed during a short period at OCV and/or reordering of the Ru during OCV.

The results indicate that there is no difference in durability between the pure Pt and the PtRu anodes, e.g. the first 2,500 test hours for MEA 1645 & MEA 1647 (Fig. 10). However, experimental mistakes/failures make it difficult to make solid conclusions.

3.3 CONCLUSION ON LT PEM LIFETIME AND DURABILITY

The decay rate observed at steady state operation is significantly higher for all MEAs than the decay rate obtained from the I-V characterisations. It is therefore concluded that the irreversible degradation is acceptable, but can be improved particularly by improving the cathode catalyst. The reversible decay can be improved by implementing 'refresh' cycles (short OCV periods) avoiding steady state operation for longer periods. This will diminish the difference between the reversible and the irreversible decay. The lowest irreversible degradation rate is 1 µV/h, which corresponds to a lifetime of 70,000 h. This is much better than the 2020 Danish Road Map target for MEAs.

4. DMFC

4.1 INTRODUCTION

The direct use of liquid fuel has made the DMFC technology attractive as an alternative to batteries. DMFC systems are expected to outperform their primary market competitors, lithium-ion batteries in particular, at sufficient long operating hours. However, durable operation and the ability to deliver the required power for several thousands of hours are crucial for a commercial success of DMFCs. However, the DMFC durability is not well established. The presented work within this project represents some if not the longest DMFC tests reported.

4.2 DMFC SINGLE CELL TESTS

Four (4) DMFC single cells has been long-term tested (in total for 27,600 test hours) under controlled environment in the laboratory. Three (3) different test protocols has been applied. The main difference between the applied test protocols are the frequency and time of the current interruptions i.e. the DMFC MEA is exposed to current interruption for 0.03% of the time at protocol 1, 20% of the time at protocol 2, and 5.8% of the time at protocol 3. The test protocol 3 is defined as close to IRDs DMFC module operational pattern as possible, the only difference is that the single cell is operated with a constant fresh fuel supply while the MeOH-water is re-circulated in the module, having a variable MeOH concentration. Test protocol 2 was defined as an AST as the MEA frequently is exposed to OCV. Test protocol 1 & 2 were formulated to investigate the effect of minimizing and extending the current interruption refresh cycles applied in the DMFC-module. The use of current interruption refresh cycles has previously been shown to be beneficiary judged by the cell voltages, but the length and frequency of the cycles were not established.

The applied catalyst loadings and test protocols of the single cell DMFC MEAs tested is listed along with the main results in Table 10. Examples on the measured long-time performance of the tested cells are shown in Fig. 18-19. The MEA tested after test protocol 2 proved to be more durable than expected (the test protocol did not prove to be truly accelerated). MEAs tested after test protocol 1 & 2 show a temporary performance increase every 250 hours where the characterisation takes place. The listed degradation rate in Table 10 is based on linear regression of all data. The low catalyst loaded MEA tested by Protocol 1 (W05A120609C) shows a significant lower degradation than the higher catalyst loaded MEA (W44A120209C). It is furthermore noteworthy that only 10% of the BoL voltage is lost although the catalyst loading is reduced by 40%. The degradation rate for the MEA tested after protocol 2 (W05A120609C) and 3 (W04A030211A) is almost twice as high as the lowest degradation observed for the MEA tested after protocol 1 (W05A120609C). The lowest degradation rate indicates a lifetime potential well in-line with the national Danish road map target for 2012 (Table 1 & 10).

Table 10 List of the tested single cell DMFC MEAs and summary of the results.

MEA ID	Test Protocol	U_{BoL} V	@ I A/cm^2	Test hours	Degradation rate µV/h	Anode Catalyst Loading mg PtRu/cm^2	Cathode Catalyst Loading mg Pt/cm^2
W44A120209C	01	0.429	0.20	10,024	11.8	3.5	1.6
W05A120609C	01	0.390	0.20	8,773	8.5	1.8	1.3
W05A120209A	02	0.393	0.20	5,053	14.5	1.9	1.3
W04A030211A	03	0.376	0.25	3,750	15.6	1.8	1.3

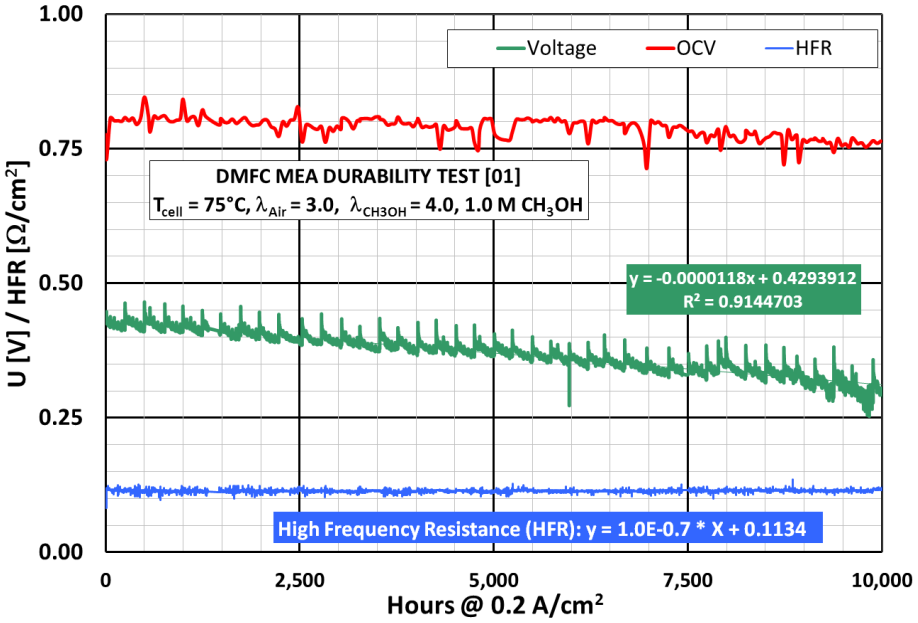

Fig. 18 Long-term single DMFC cell test (MEA: W44A120209C) tested after test-protocol 1.

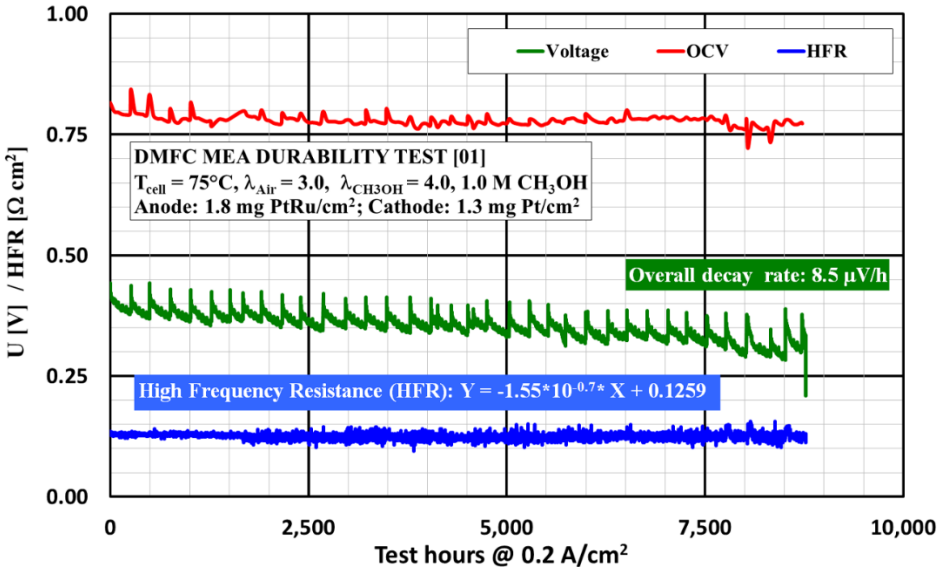

Fig. 19 Long-term single DMFC cell test (MEA: W05A120609C) tested after test-protocol 1.

Selected results of the characterization is shown in Fig. 20-21. The ≈35% decrease of the active cathode catalyst is significant, while the indicated decrease of the anode catalyst surface area not is significant. The degradation observed at constant load is partly related to loss of active cathode ECSA, as all MEAs show an increase in the ohmic resistance (Fig. 21).

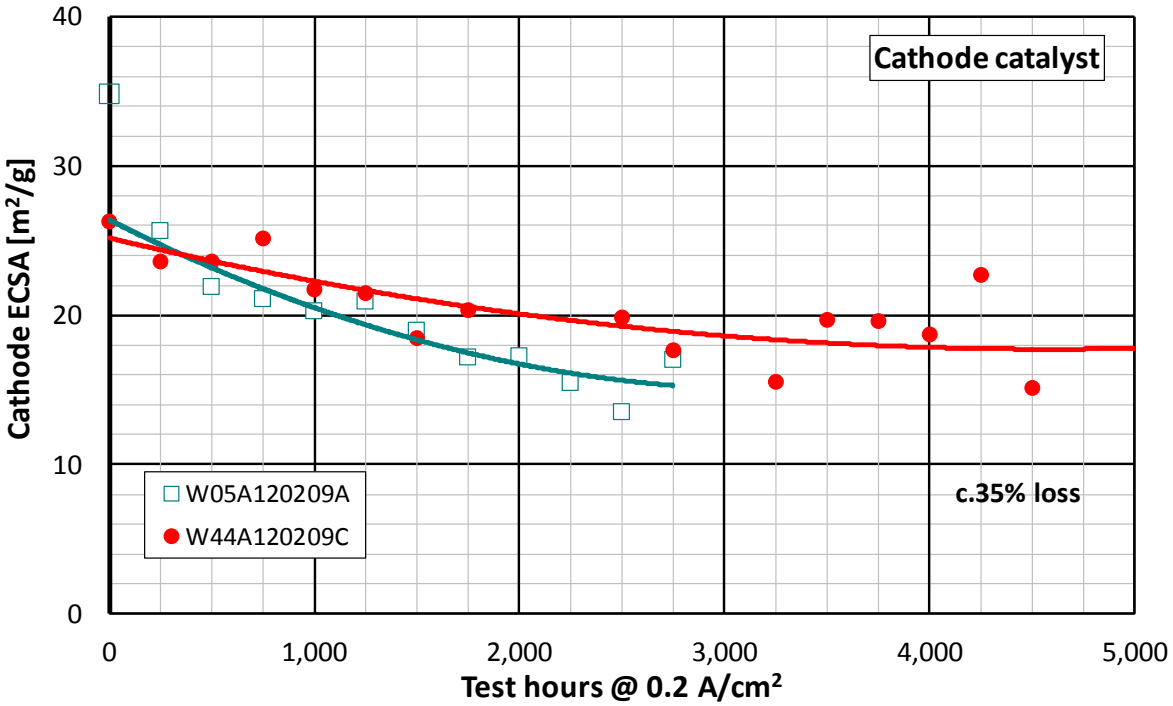

Fig. 20 Examples of measured cathode ECSA loss for two (2) MEAs tested after test protocol 1 (W44A120209C) and 2 (W05A120209A), respectively.

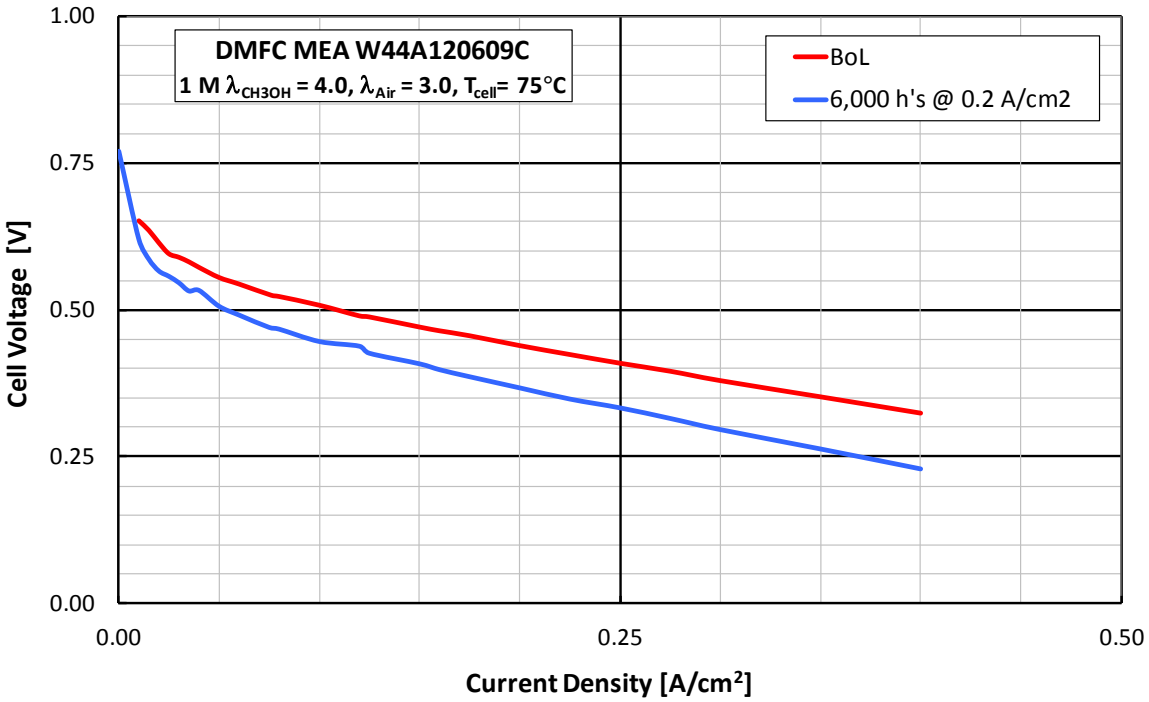

Fig. 21 Measured performance loss versus current density for MEA W44A120209C tested after protocol 1.

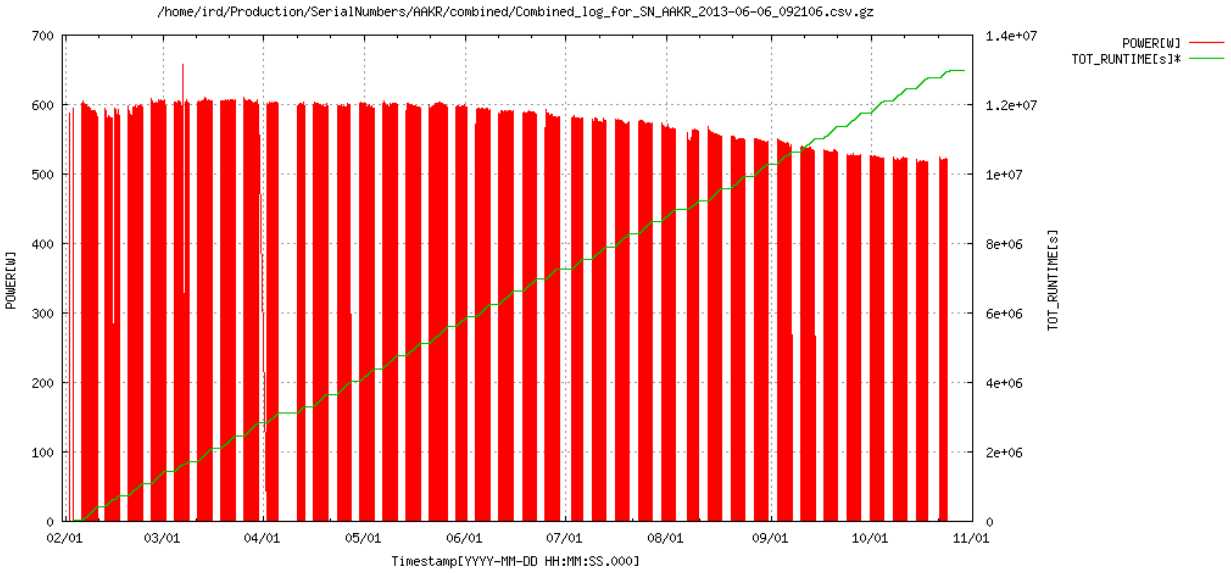

Fig. 22 Stress test with frequent cold start/stop and continuous runtime in a DMFC module, Test pattern: 120 Hours On followed by 48 Off, Runtime: 3,611 hours / Real time: ~6,500 hours.

4.3 DMFC STACK TESTS

Overall the DMFC stacks have been operated ~7,500 hours in total in the period of the project. One stack has been operated for 3,600 hours with an average degradation of 14 µV/h two other stacks have been operated for 1,900 hours and 2,000 hours, these test where however affected by external factors and thus the degradation rates where significantly higher than expected.

Analysis of the stack that operated 3,600 hours (Fig.22) in the system showed that 50% of the best MEA's had a degradation of 8.1 µV/h on average, this exceed the national roadmap targets for 2012 and almost reaches the 2014 roadmap targets for stacks (see Table 1). Some of the MEAs did not have any measurable degradation thus the potential for 10,000 hours of operation in a DMFC stack is within reach.

4.4 POST MORTEM OF DMFC MEAS

SEM pictures of fresh and tested DMFC MEAs is shown in Fig. 23. It is evident from the comparison that the anode is very uneven even in the fresh MEA, and that the cathode for MEA W04A030211A (test protocol 3) is much damaged. The membrane for sample W44A120209C (test protocol 1) is slightly thinned compared with the fresh MEA. The measured thicknesses for MEA W04A030211A indicate an oblique cut and cannot be used for solid conclusions. The associated EDX analyses shows that significant traces of Ru from the anode can be found on the cathode catalysts, and that part of the anode is depleted in Ru (the original weight proportion Pt:Ru is 2) particular at the air inlet.

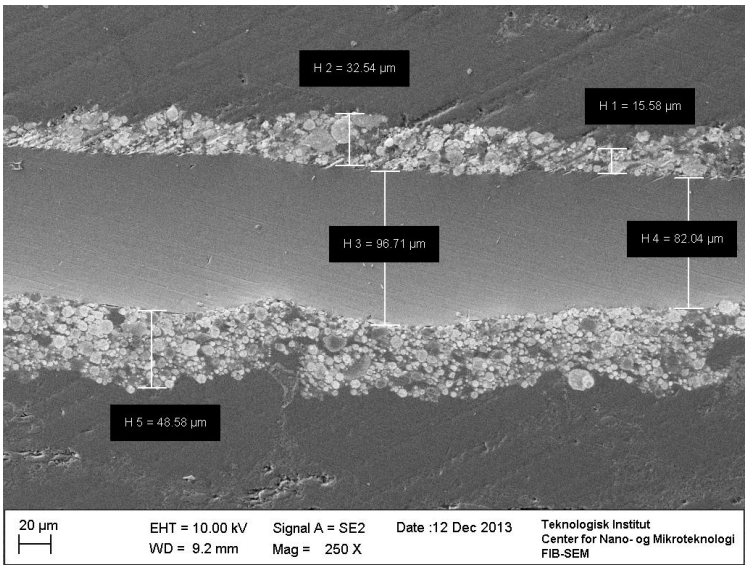

Fresh DMFC MEA

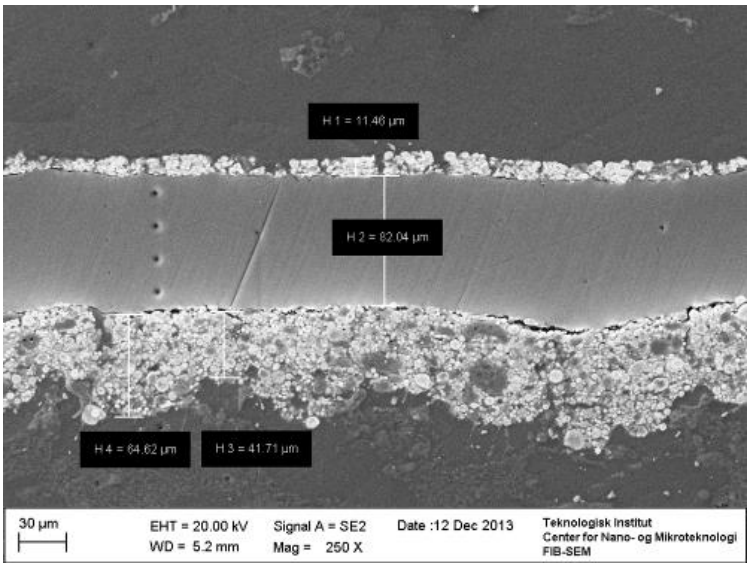

Post mortem pictures of MEA W44A120209C (cf. Table 10), single cell tested for +10,000 hours

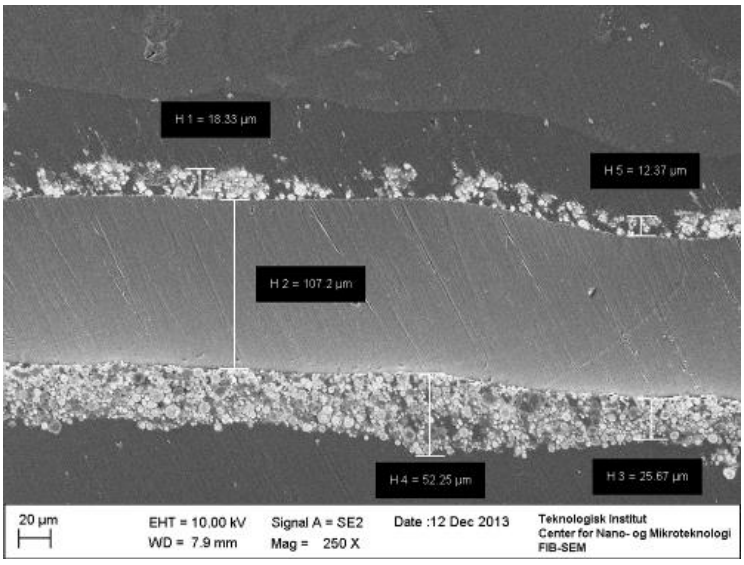

Post mortem pictures of MEA W04A030211A (cf. Table 10). Single cell DMFC MEA tested in system mode for 3,750 hours

Fig. 23 SEM picture of a fresh 'virgin' DMFC MEA and tested DMFC MEAs.

4.5 CONCLUSION ON DMFC LIFETIME AND DURABILITY

Four (4) DMFC single cells has been long term tested (in total for 27,600 test hours) under controlled environment in the laboratory. Three (3) different test protocols has been applied. The main difference between the protocols is related to the length and frequency of the refresh cycles that implies current interruption. The results show that the best MEA possessed an average degradation rate of 8.5 µV/h over the 8,773 hours tested. This is well in-line with the national Danish road-map lifetime target for 2012 which is 8 µV/h[vi]. The other tested MEAs possessed higher degradation rates ranging from 12 to 16 µV/h. The intermediate characterisations illustrate a significant loss of cathode ECSA (≈35%), but no significant membrane crossover development nor anode catalyst coarsening. The MEAs have after EoT been characterised for microstructural changes (SEM) and element redistribution (EDX) at the Danish Technological Institute. The microstructural characterisation show a significant alteration of the cathode that are markedly thinned and locally totally corroded/missing. Traces of Ruthenium is detected on the cathode, showing that MeOH and Ru crossover from the anode towards the cathode goes hand-in-hand. A significant Ru-depletion is detected on the anode air-inlet location. The obtained results have been used to successfully optimise the operational strategy of IRDs DMFC-module.

Overall the DMFC stacks have been operated ~7,500 hours in total in the period of the project. One stack has been operated for 3,600 hours with an average degradation of 14 µV/h. Analysis of the stack that operated 3,600 hours showed that MEA's in one of the two fuel circuits possessed a degradation of 8.1 µV/h on average, this exceed the national roadmap targets for 2012 and almost reaches the 2014 roadmap targets for stacks.

[vi] No lifetime target is defined for 2013

5. HT PEM

5.1 INTRODUCTION

Focus in the project has been durability measurement of well know MEAs to figure out there behaviour under different operating conditions, with the aim of gaining a broader understanding of the degradation mechanisms of HT-PEM fuel cells.

This has been accomplished by running a durability test matrix, composed of different load conditions and temperatures.

Based on the knowledge gained from these measurements the existing MEAs have been optimized and a number of different new materials have tested as well.

5.2 STRATEGIC CONCEPTS

Based on literature studies the main degradation mechanism found in HT-PEM fuel cells are:

- Membrane degradation due to stress and oxidation
- Membrane loss of ionic conductivity
- Catalyst degradation due to corrosion of catalyst support.

These issues have been further investigated in the project and addressed

5.3 MATERIAL DEVELOPMENT AND ACCELERATED LIFETIME EVALUATION

This task has been carried out in close collaboration with other parallel national projects, that the partners have been involved in most importantly the HotMEA projects and the Catbooster project (both supported by Energinet.dk). The testing and the evaluation of the developed materials have been done in the framework of the present DuRaPEM project.

5.3.1 TEST SETUPS

The 12 cell test setup build during the previous durability project has supplement by an extra 12 cells, incorporating lessons learned when building the first 12 cells (Fig. 24). At the end of the project 24 continuously operated cells, running under simple constant load are available allowing for a large number of measurements, to ensure reproducibility and allow for long term testing. At the end of the project the DTUs testing capabilities consists of:

12 single 10 cm^2 test cells all capable of:

- Temperatures from 25–200°C
- Constant current mode running 0–10 A (1 A/cm^2)
- Constant voltage mode
- Hydrogen flows up to lambda 2 at max current
- Air flows up to lambda 2 at max current

12 single 10 cm^2 test cells all capable of:

- Temperatures from 25–200°C
- Constant current mode running 0 – 20 A (2 A/cm^2)
- Constant voltage mode
- Hydrogen flows up to lambda 2 at max current
- Air flows up to lambda 5 at max current
- Over potential measurements are

possible as well

Fig, 24 24 cells durability test setup, for long term testing

5.3.2 MEMBRANE DEVELOPMENT

A number of new membrane materials have been tested in the project, with the aim of improving both the chemical stability, the long term durability and proton conductivity.

The most important results are summarized below.

5.3.2.1 Different molecular weight PBI

Generally, the commercially available PBI polymer (Celazole, Celanese) has a low to medium linear molecular weight ranging from about 23 – 37 kDa. However, PBI membranes with lower molecular weights give poor mechanical stability and oxidative resistance.

A higher molecular weight PBI is desired but if the molecular weight gets too high the solubility of the polymer decreases making it impossible to manufacture solutions of PBI to cast membranes from.

The proton conductivity of PA doped PBI membranes highly depends on the acid doping level (ADL) of the membranes, defined as the mole number of PA per molar repeating unit of the polymer. For example, the conductivity of PBI membranes at 160°C is typically around 0.02 S cm^{-1} for ADLs of 5-6, and it increases to 0.10 S cm^{-1} as ADLs increases to ca. 10. The increased PA content in the membrane generates a dynamic hydrogen bond networks among phosphoric acid molecules, which facilitate the proton transfer via a hydrogen bond breaking and forming processes.

A number of different molecular weight PBI membranes were tested for chemical stability, mechanical stability and made in to MEAs for fuel cell testing.

In general both the oxidative and mechanical strength increases with molecular weight and higher molecular weight PBI allows for higher doping levels.

The fuel cell test results are summarized in Fig. 25. The membrane stability of the reference membrane and a thermally cured membrane is shown in Fig. 26.

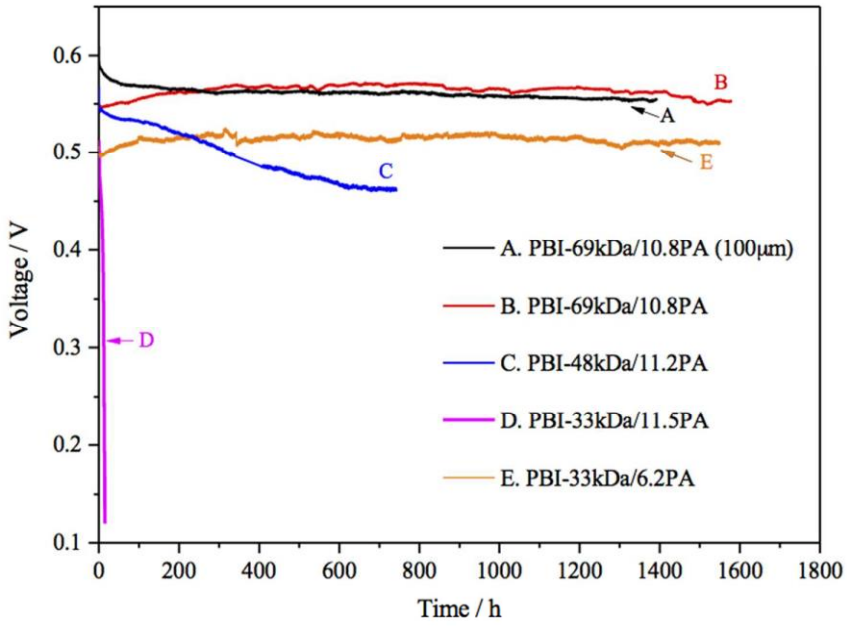

Fig. 25 Fuel cell voltages at 300 mA cm^{-2} as a function of time for MEAs based on acid doped PBI membranes with different molecular weights at 160°C. No humidification was used for either H_2 nor air. The catalyst loading was 0.6 mg Pt cm^{-2} for each electrode. The membrane thicknesses were around 140 μm except one of 100 μm as specified in the figure.

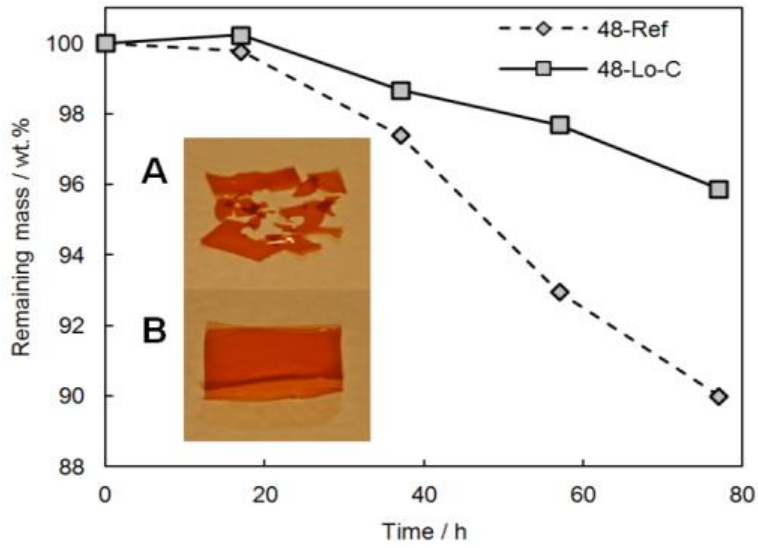

Fig. 26 Remaining membrane mass after certain durations of the Fenton test of the non-cured reference membrane (48-Ref) and of the membrane that had been cured at 350°C for 16 h under argon (48-Lo-C). The insert is a photographs of 48-Ref (A) and 48-Lo-C (B) after 80 h Fenton test

5.3.3 ELECTRODE DEVELOPMENT

Work has continued on modified supports for Pt catalyst. For catalyst evaluation, a potential cycling protocol will be adapted between 0.6 V and 1.2 V versus RHE in H_3PO_4 at temperature of 150°C.

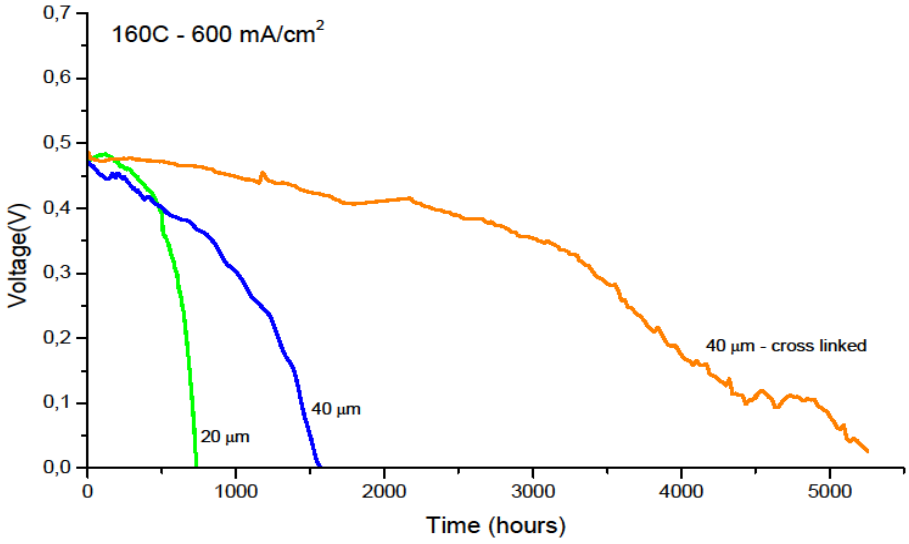

Fig. 27 Fuel cell voltages as a function of time for the MEAs based on non-cured PBI (blue and green lines) and PBI that had been cured at 350°C for 16 h under argon (orange line) prior to the acid doping. The cells were operated at a current load of 600 mA cm^{-2}. The corresponding membrane thicknesses are indicated in the figure.

Table 11 The accomplish HT PEMFC single cell test matrix.

Temp/load	227 mA/cm²		681 mA/cm²		909 mA/cm²	
120°C	20 µm					
140°C	20 µm	40 µm	20 µm	40 µm	20 µm	
160°C	20 µm	40 µm	20 µm	40 µm	20 µm	40 µm
180°C	20 µm	40 µm	20 µm	40 µm	20 µm	

5.4 Optimise MEAs and FC components

5.4.1 Durability matrix

During the project a durability matrix has been tested, with the overall idea to establish a baseline for comparison of future improvements and to determine the correlation between measurements at different conditions. The goal is to determine which single measurements could be used as standards for testing improvements in manufacturing, relating to performance, and how this would affect the overall performance at all conditions.

The test matrix (Table 11) was completed for both 20 µm and 40 µm thick membranes. The original test matrix comprised more experiments at 120°C, but these experiments quickly proved not to contribute to more knowledge than the results obtained at 140ºC. Furthermore, the low temperature setting is of less importance as the MEA at this temperature still is very sensitive towards fuel contaminants.

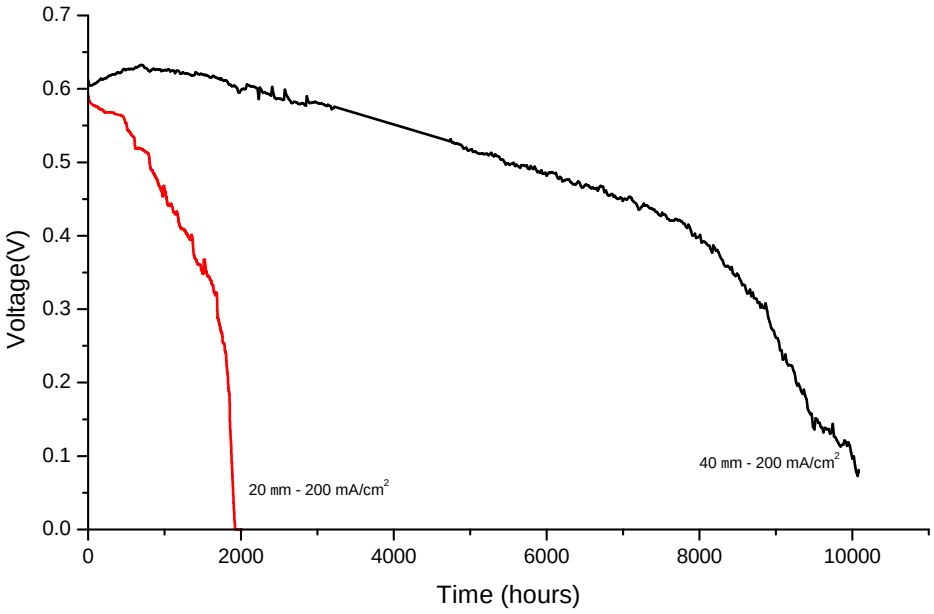

Fig. 28 Effect of thickness, 20 µm and 40 µm membranes run at constant current of 227 mA/cm^2. Pt loading: anode 0.3 and cathode 0.6 mg/cm^2. Temperature: 160ºC Reactants: H_2/Air 1/1 bar, Area: 8.8 cm^2.

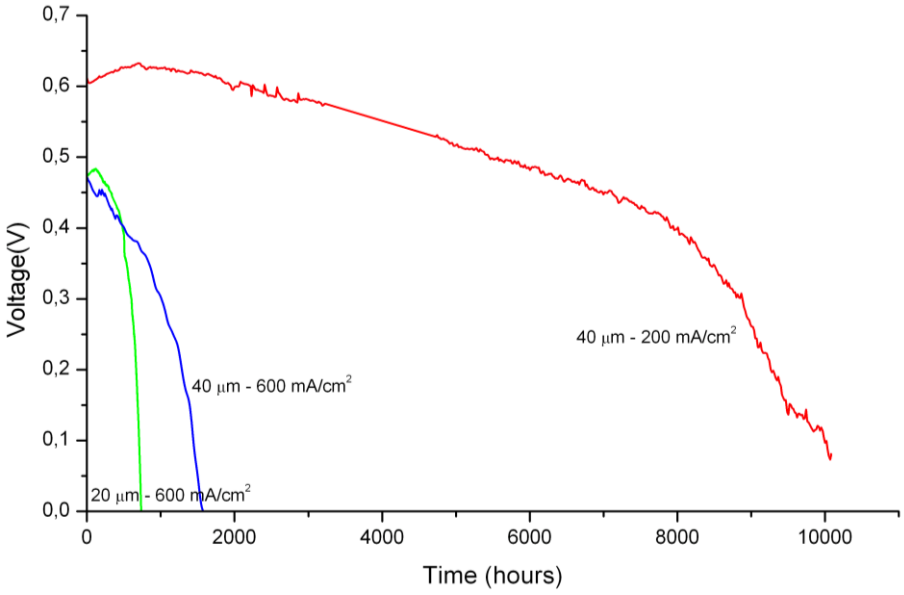

Fig. 29 Effect of current density, measurements at 227 mA/cm^2 and 681 mA/cm^2 (current density in the figure is rounded). Pt loading: anode 0.3 and cathode 0.6 mg/cm^2. Temperature: 160ºC. Reactants: H_2/Air 1/1 bar, Area: 8.8 cm^2.

The 20 µm membranes were tested since it was the hope that a thinner membrane would decrease the membrane resistance and improve performance. However, the tests showed that the thinner membrane did not result in any significantly higher performance, and the overall durability was considerably lower (Fig. 28-30). The reason for the lower durability is that the thinner membranes are not able to hold the acid as strongly as the thicker membranes.

Increasing the current density results in a significant decrease in durability (Fig. 30). The same is true for increased temperature (Fig. 31).

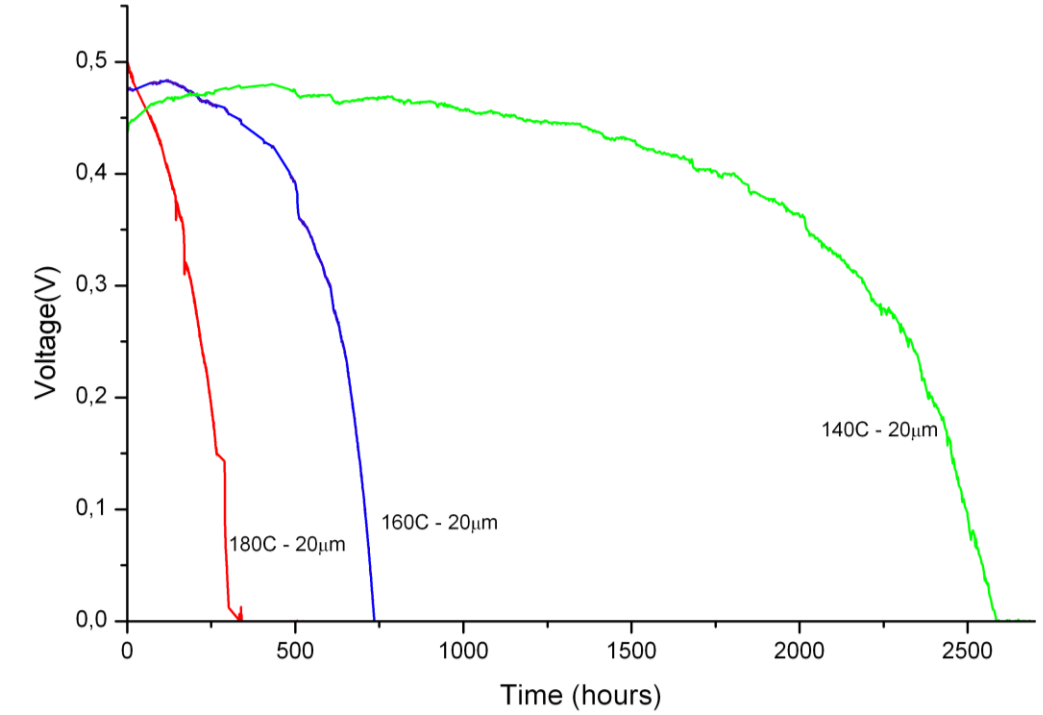

Fig. 30 Effect of temperature. Cells running at a constant load of 681 mA/cm^2. Pt loading: anode 0.3 and cathode 0.6 mg/cm^2 Reactants: H_2/Air: 1/1 bar, Area: 8.8 cm^2

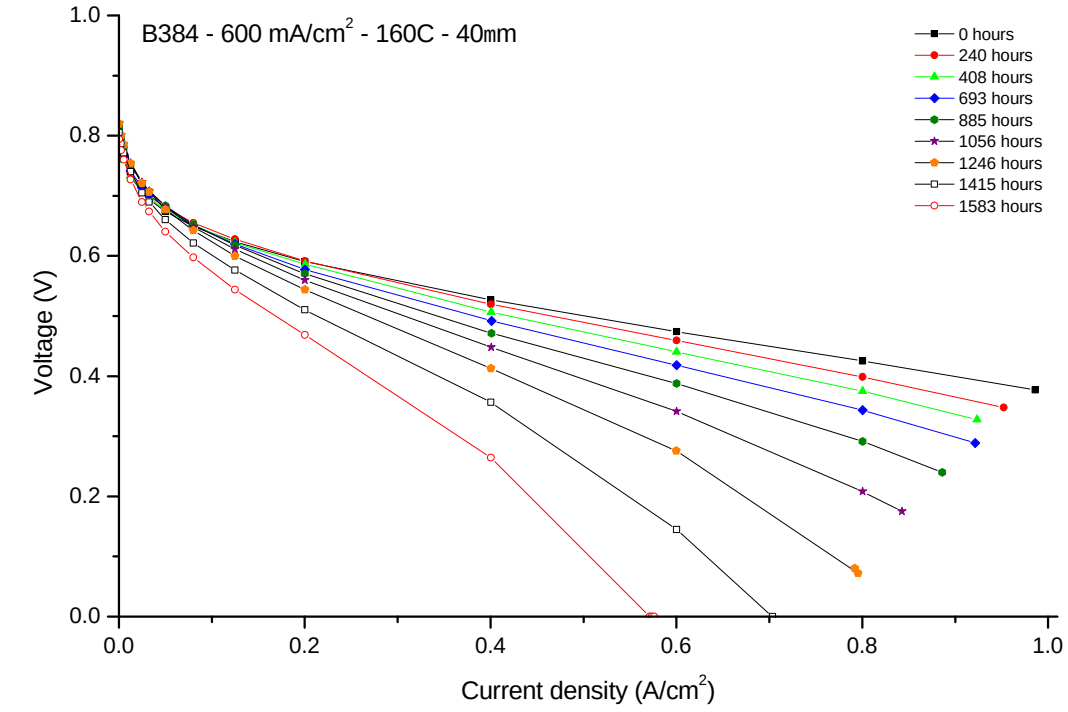

Fig. 31 Typical development of polarisation curves over time. Pt loading: anode 0.3 and cathode 0.6 mg/cm^2. Reactants: H_2/Air 1/1 bar, Area: 8.8 cm^2

5.4.2 CONCLUSIONS

The durability matrix gave the following conclusions

- Under steady state conditions the main degradation comes from the membrane
- Catalyst degradation is mainly observed during start and stop cycling
- The reason for degradation is a loss of MEA conductivity over time that accelerates just before EoL.
- Biggest improvement in durability has come from improvement in manufacturing of the existing MEAs
  - Higher uniformity of the membrane results in longer lifetime
  - Control of doping level improve durability
- Acid management is key to improving the membrane performance

Running at higher current densities significantly decreases durability, which is believed to be due to local heating of the

5.4.3 POST MORTEM ANALYSIS

A number of cycling test were also performed to specifically stress the catalyst. The MEAs were cycled from 0.9–1.2 V for a number of cycles and post mortem analysis were performed on the catalyst layers.

The difference between standard Vulcan XC 72R support (VXC), graphitized Vulcan XC-72 (G-VXC) and carbon nanotubes (CNT) supports have been studied.

SEM and TEM images of MEAs and the electrodes were performed before and after testing (Fig. 32-34).

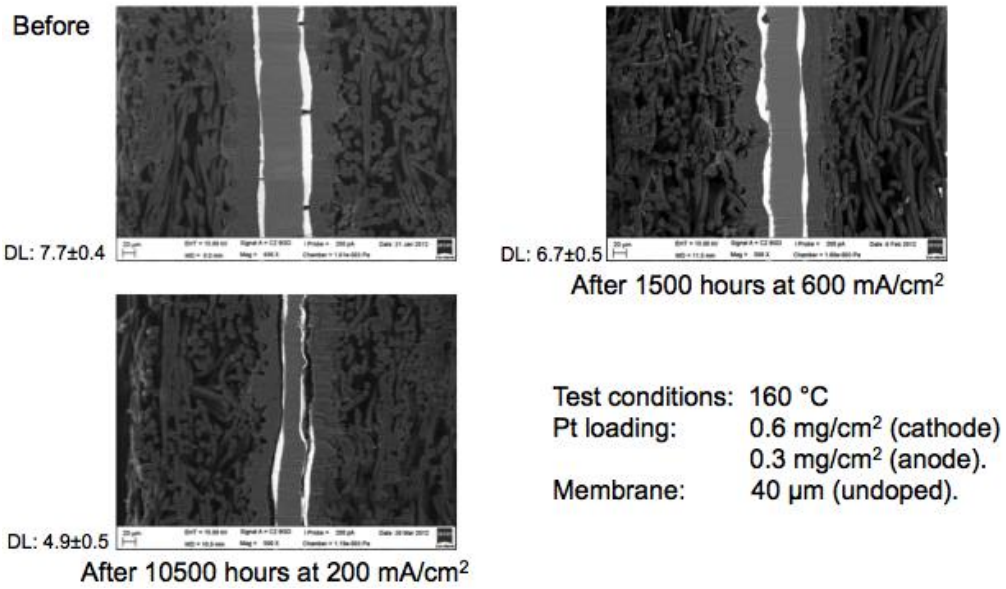

Fig. 32 Backscatter SEM image before a after running a durability matrix cell

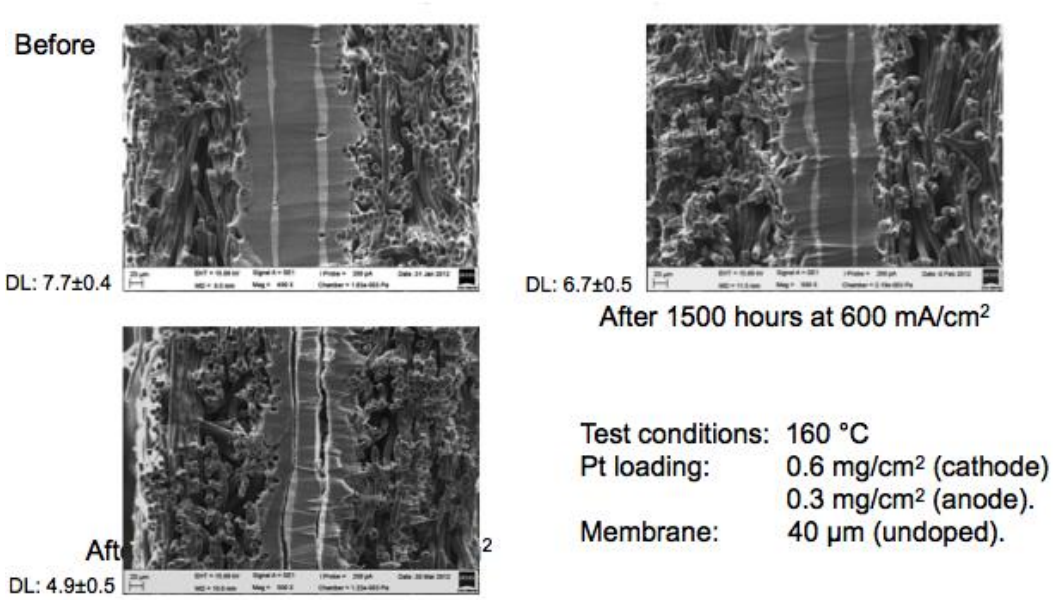

Fig. 33 SEM pictures.

Table 12 BET area changes of the catalyst samples estimated from the XRD measurements during the potential cycling tests. The first set of data is from a previous work.

Catalysts		Pt particle size (nm)	Estimated surface area (m^2/g)	Calculated performance loss (mV)
39% Pt/VXC	Before test	3.6	39.3	0
	Anode, after 3.5 years	8.3	12.6	44.3
	Cathode, after 3.5 years	11.1	16.9	59.3
39% Pt/VXC	Before test	4.0	34.9	0
	Anode, after 3200 cycles	6.4	16.5	24.5
	Cathode, after 3200 cycles	8.5	21.8	39.3
39% Pt/G-VXC	Before test	5.7	24.7	0
	Anode, after 3350 cycles	7.2	19.5	13.1
	Cathode, after 3350 cycles	8.3	16.9	20.0
39% Pt/CNT	Before test	2.8	47.7	0
	Anode, after 3159 cycles	3.5	39.6	9.7
	Cathode, after 3159 cycles	4.5	32.7	19.6
	Anode, after 4355 cycles	3.8	36.5	13.9
	Cathode, after 4355 cycles	4.9	29.9	24.3

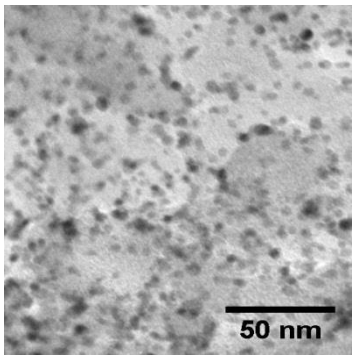

Pt/C, before test

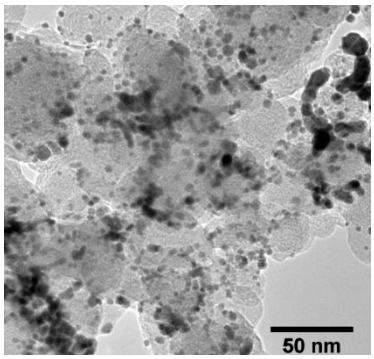

Pt/C, anode after test

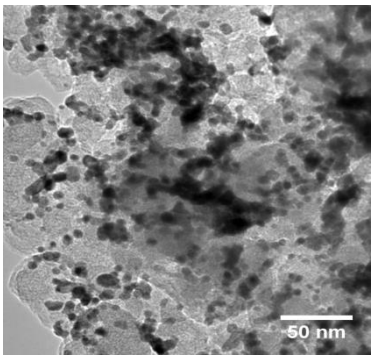

Pt/C, cathode after test

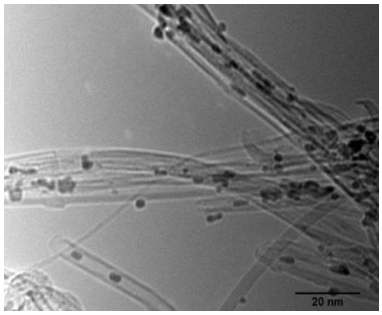

CNT, before test

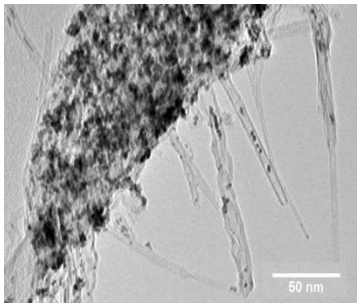

CNT, Anode after test

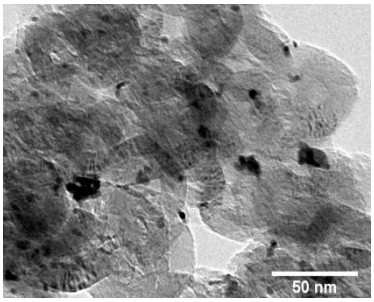

CNT, Cathode after test

Fig. 34 The TEM photographs of catalysts supported on VXC (3200 cycles) and CNT (3159 cycles) as anode and cathode before and after the potential cycling tests.

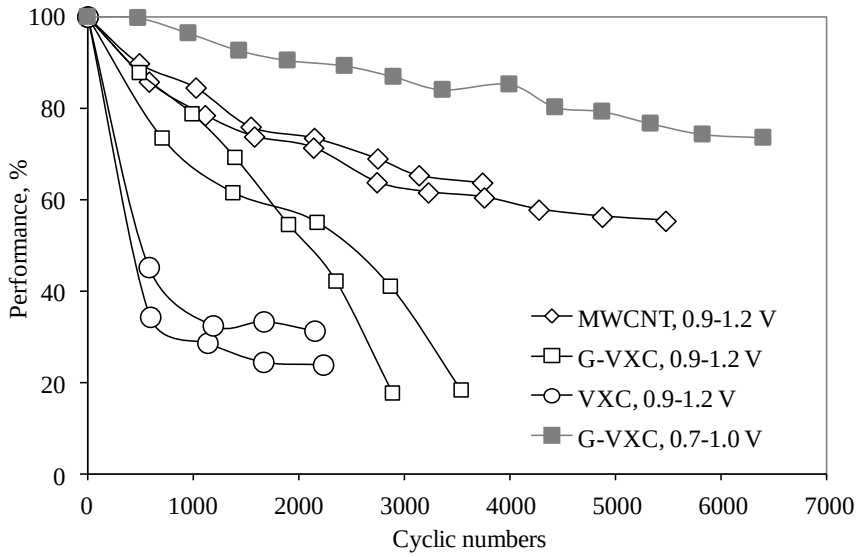

Fig. 35 Fuel cell performance degradation in term of the relative current density at 0.5 V during the potential cycling tests between 0.9 and 1.2 V (open symbols) or between 0.7 and 1.0 V (solid symbols) at 150°C. The cathode catalysts were prepared from different types of carbon supports as indicated in the figure.

Over time a significant drop in performance is seen during this accelerated test, see Fig. 35, the CNT performed the best, with the graphitized Vulcan also showing significant improvements. For comparison a cycling test running from 0.7 -1 V was also included, showing how this form of

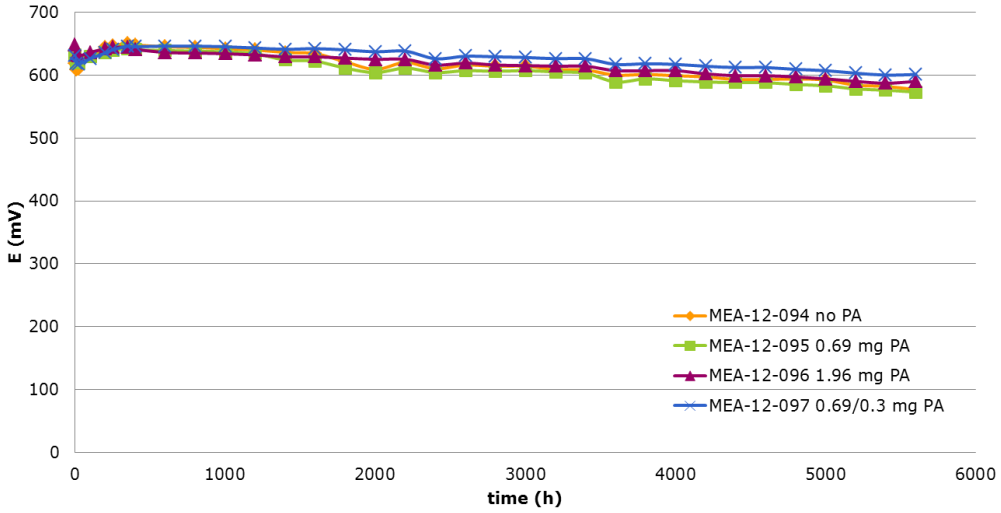

Fig. 36 Durability of optimised MEAs. Running under constant current of 238 mA/cm^2.

degradation can be significantly reduced by preventing the cell from raising high potentials during start up and shutdown.

The degradation of catalysts supported on different carbon materials in high temperature PBI cells was investigated under the accelerated potential cycling tests at 150°C. As the major mechanism of the fuel cell performance degradation, the ECSA of the cathodic catalysts was monitored by cyclic voltammetry, showing a steady decrease during the accelerated potential cycling tests, which was also confirmed by the post TEM and XRD analysis. The fuel cell performance degradation under the accelerated potential cycling test showed strong dependence on the catalyst sup- ports. Heat treatment of the carbon black improved the stability and therefore the catalyst durability though at the expense of a significant decrease in the specific surface area. Multi-walled carbon nanotubes as catalyst support showed further significant improvement in the catalyst and fuel cell durability.

5.4.3 Optimized MEAs

Based on the results obtained and the conclusions drawn from these new MEAs were manufactured and tested[36]. They incorporated the following features to ensure better durability:

- Cross linked PBI, DL 8
- Controlled amounts of acid in the catalyst layer
- Higher Pt loading, up to 1.5 mg/cm^2

Results for the optimized catalyst support were not incorporated in the test.

Durability result from the optimized MEAs is shown in Fig. 36. Degradation rates are lowered to 5.7 µV/h for the optimised MEAs, which is lower than half of the degradation rate obtained with SoA MEAs (≈13 µV/h).

5.5 Conclusion on HT PEM Lifetime and Durability

By modifying the manufacturing process and the membrane of the MEAs significant improvements in durability have been obtained.

Lesson from the large number of tests (more than 70 cells have been run for extended periods of time) are that the uniformity of the MEAs play a significant role in durability.

During the project the MEAs produces have seen a significant improvement in membrane thickness variations from ±10 µm, down to ±2 µm with can be directly read in the durability of the MEAs.

Better control of the assembly procedure for the MEAs has also results in improved durability.

Over all the project has resulted in a better understanding of the degradation mechanisms, primarily the main degradation mechanism being the loss of ionic conductivity over time. This work will be continued in the DuraPEM III project were the exact reasons for this will be further studied.

6. DISSEMINATION

The project results have been disseminated in a number of peer-reviewed papers and at several scientific conferences, as listed below.

PUBLICATIONS IN PEER-REVIEWED PAPERS:

Aili, D; Cleemann, LN; Li, Q; Jensen, JO; Christensen, E & Bjerrum, NJ (2012): Thermal curing of PBI membranes for high temperature PEM fuel cells. J. of Materials Chemistry 22(12)5444–5453

Ali, ST; Li; Q; Pan, C; Jensen, JO; Nielsen, LP & Møller, P (2011): Effect of chloride impurities on the performance and durability of polybenzimidazole-based high temperature proton exchange membrane fuel cells. Inter. J. Hydrogen Energy 36(2)1628-1636

Andersen, SM; Grahl-Madsen, L; Skou, EMI (2011): Studies on PEM Fuel Cell Noble Metal Catalyst Dissolution**.** Solid State Ionics 192(1)602-606

Andersen; SM; Borghei, M; Lund, PL; Elina, Y-R; Pasanen, A; Kauppinen, E; Ruiz, V; Kauranen, P & Skou, EM (2013): Durability of carbon nanofiber (CNF) & carbon nanotube (CNT) as catalyst support for Proton Exchange Membrane Fuel Cells. Solid State Ionics 231, 94–101

Cleemann, LN; Li, Q; Jensen, JO; Pan, C; Liu, CD; Dai, S & Bjerrum, NJ (2013): Catalyst Degradation in High Temperature Proton Exchange Membrane Fuel Cells Based on Acid Doped Polybenzimidazole Membranes. Fuel Cells (on-line DOI: 10.1002/fuce.201200186)

Liao, J; Li, Q; Rudbeck, HC; Jensen, JO; Chromik, A; Bjerrum, NJ; Kerres, J & Xing, W (2011): Oxidative degradation of polybenzimidazole membranes as electrolytes for high temperature proton exchange membrane fuel cells. Fuel Cells 2011, 11(6)745-55

Nørgaard, CF; Stamatin, SN; Larsen, MJ & Skou, EM (Publication pending until patent has been granted): Redeposition of electrochemically dissolved platinum as nanoparticles on carbon

Yang, J; Li, Q; Cleemann, LN; Xu, C; Jensen, JO; Pan, C; Bjerrum, NJ & He, R (2012): Synthesis and properties of poly(aryl sulfone benzimidazole) and its copolymers for high temperature membrane electrolytes for fuel cells. J. of Materials Chemistry 22(22)11185–11195

Yang, J; Li, Q; Jensen, JO; Pan, C; Cleemann, LN ; Bjerrum, NJ; He, Ronghuan (2012): Phosphoric acid doped imidazolium polysulfone membranes for high temperature proton exchange membrane fuel cells. J. of Power Sources vol. 205, pp. 114-121

OTHER PUBLICATIONS:

Li, Q; Aili, D; Rudbeck, HC; Jensen, JO & Bjerrum, NJ (2011): Polybenzimidazoles – Synthesis, Membranes and Applications for Energy Conversion. Book Chapter in Advanced Materials Research, Nova Science Publishers, Inc.

Skou, EM, Stamatin, SN & Nørgaard, CF (applied): Method for recovering platinum group metals from catalytic structures. Patent application in progress

ORAL AND POSTER PRESENTATIONS:

Cleemann, LN; Li, W; Jensen, JO & Aili, D (2012): Durabiltity of HT-PEM fuel cells. Invited lecture at 1st International Expert Workshop, High Temperature PEM fuel cells, ZBT Duisburg, Germany

Hjuler, HA; Steenberg, T; Rudbeck, HC; Cleemann, LN; Li, Q; Jensen, JO & Bjerrum, NJ (2010): Development and Characterizations of High Performance MEAs For High Temperature PBI Fuel Cells. PROGRESS MEA 2010, Palais des Congrès, La Grande Motte, France, 19-22 Sept 2010

Jensen, JO; Li, Q; Pan, C & Bjerrum, NJ (2010): Ongoing Efforts Addressing Degradation of High Temperature PEMFC. Oral and extended abstract at 18th World Hydrogen Energy Conference 2010 (WHEC2010), Essen, May 16-21 2010.

Jensen, JO; Li, Q; Pan, C; Rudbeck, HC; Steenberg, T & Bjerrum, NJ (2010): Recent advances with high temperature PEMFC in Denmark. 8th International Symposium on New Materials for Electrochemical Systems, July 11-15, 2010, Shanghai, China. (2010) (Invited keynote)

Jensen, JO; Olsen, MI; Li, Q; Vasilliev, A; Pan, C; Steenberg, T & Bjerrum, NJ (2010): A direct DME fuel cell based on acid doped PBI. Oral presentation at PROGRESS MEA 2010, Palais des Congrès, La Grande Motte, France, 19-22 Sept 2010

Kerres, J; Li, Q, Rudbeck, HC; Chromik, A; Jensen, JO; Pan, C; Steenberg, T; Calverley, M & Bjerrum, NJ (2010): Properties, Degradation and High Temperature Fuel Cell Test of Different Types of PBI and PBI Blend Membranes. PROGRESS MEA 2010, Palais des Congrès, La Grande Motte, France, 19-22 Sept 2010

Li, Q; Aili, D; Jensen, JO; Cleemann, LN; Rudbeck, HC; Steenberg, T; Hjuler, HA & Bjerrum, NJ (2011): Polybenzimidazole based HT-PEMFC: Recent progress in material development and durability evaluation. Oral presentation at Hydrogen & Fuel Cells 2011, May 15 – 18, 2011, Vancouver, BC, Canada

Li, Q; Jensen, JO; Pan, C; Liao, JH; Rudbeck, HV; Cleemann; LN & Bjerrum, NJ (2010): Durability Issues and Status of High Temperature Proton Exchange Membrane Fuel Cells Based on Acid Doped Polybenzimidazole Membranes, Abstract and oral presentation at the 217th Electrochemical Society Meeting, April 25 - 30, 2010, Vancouver, Canada

Li, Q; Jensen, JO; Rudbeck, HC; Liao, JH; Cleemann, LN; Chromik, A; Kerres, J & Bjerrum, NJ (2010): Polymer Degradation and Catalyst Sintering in High Temperature PEMFC Based on Acid Doped Polybenzimidazole Membranes, abstract submitted to PROGRESS MEA 2010, Palais des Congrès, La Grande Motte, France, 19-22 Sept 2010

Nørgaard CF, Larsen MJ, Andersen SM, Skou EM, "Electrochemical recovery of platinum from PEM fuel cell electrodes", June 22nd 2012, Poster presented at "The Energy & Materials Research Conference 2012, Torremolinos, Málaga, Spain

Odgaard, M & Grahl-Madsen, L (2011): DMFC durability. Oral presentation at the 2nd International workshop on Degradation Issues in Fuel Cells. Thessaloniki, Greece, 21-23 of September, 2011

Odgaard, M (2010): Durability and performance of MEAs in the commercial fuel cell applications. Oral presentation at the 'Fuel cell durability & performance conference', Boston December 9-10, 2010

7. REFERENCES

[1] T. Payne, [Fuel] Cells Durability & Performance, The Knowledge Press Inc., US Brookline, 2009

[2] Q.F. Li, J.O. Jensen, R.F. Savinell and N.J. Bjerrum, Progress in Polymer Science, 34(5) 449-477, (2009)

[3] T.J. Schmidt, J. Baurmeister, ECS Transactions 3 (2006) 861; J Power Sources 176 (2008) 428

[4] Oono, Y; Sounai, A; Hori, M, J. Power Sources, 210, 366-373 (2012)

[5] Wu, J; Yuan, XZ; Martin, JJ; Wang, H; Zhang, J; Shen, J; Wu, S & Merida, W (2008): A review of PEM fuel cell durability: Degradation mechanisms and mitigation strategies. J. of Power Sources 184, 104-119

[6] Jim Fletcher & Philip Cox (2011): New MEA Materials for Improved DMFC Performance, Durability, and Cost. http://www.hydrogen.energy.gov/pdfs/review11/fc064_fletcher_2011_o.pdf

[7] X_G Chin, P-Y Yan & C-P Wang (2010): Enhancement of Durability and Performance in Direct Methanol Fuel Cell by a Microporous Layer with Ultra-Small Pores. ECS Transactions 26, 295-98

[8] Shao Y., Yin G. & Gao Y. J. Power Sources 171, 558–566, 2007.

[9] Yu X. & Ye S., J. Power Sources 172, 145–154, 2007.

[10] Nieto-Marquez A., Romero R., Romero A. & Valverde J. L., J. Mater. Chem. 21, 1664-1672, 2011.

[11] Li W., Ma H., Li, X., Li W., Wu M. & Bao X., J. Phys. Chem. B 107 (26) 6292-6299, 2003.

[12] Darkrim F. & Levesque D., J. Phys. Chem. B 104 (29) 6773-6776, 2000 .

[13] Avasarala B. & Haldar P., Electrochim. Acta 55(16), 4765-4771, 2010.

[14] Andersen S. M., Grahl-Madsen L.; Skou E. M. (2011), Solid State Ionics (192)1, 602-606.

[15] Renner H. *et al*. in : Ullmann's Encyclopedia of Industrial Chemistry Vol. 28, Wiley-VCH Verlag GmbH & Co. KGaA, Weinheim, 2012, pp. 318-388.

[16] Zhao J., He X., Tian J., Wan C., Jiang C., Energy Conversion and Management 48 (2007) 450-453.

[17] Handley C., Brandon N. P., van der Vorst R., Journal of Power Sources 106 (2002) 344-352.

[18] Shore L., Matlin R., Heinz R., Efficient Process for Precious Metal Recovery from Fuel Cell Membrane Electrode Assemblies, U.S. Patent US2009/0301260 A1, 2009.

[19] Shore L., Matlin R., Heinz R., Method for Recovering Catalytic Elements from Fuel Cell Membrane Electrode Assemblies, U.S. Patent US 2010/0288079 A1, 2010.

[20] Xu F., Mu S., Pan M., International Journal of Hydrogen Energy 35 (2010) 2976-2979.

[21] Shore L., Robertson B., Anderson A., Pererson D., Benjamin T.G., DOE Hydrogen Program – FY2005 Progress Report – VII.E.2 Platinum Group Metal Recycling Technology Development, Iselin, 2005.

[22] Grot S., Grot W., Anderson A., Tyler R., DOE Hydrogen Program – FY2005 Progress Report – VII.E.1 Platinum Recycling Technology Development, New Castle, 2005.

[23] Esmaeilifar A., Rowshanzamir S., Eikani M.H., Ghazanfari E., Energy 35 (2010) 3941-3957.

[24] Topalov A.A., Katsounaros I., Auinger M., Cherevko S., Meier J.C., Klemm S.O., Mayrhofer K.J.J., Angewandte Chemie International Edition 51 (2012) 12613-12615.

[25] Meier, J.C., Galeano C., Katsounaros I, Topalov A.A., Kostka A., Schu F., Mayrhofer K.J.J., ACS Catalysis 2 (2012) 832-843.

[26] Ishimoto, T., Ogura T., Umeda M., Koyama M., The Journal of Physical Chemistry C 115 (2011) 3136-3142.

[27] Yadav A.P., Nishikata A., Tsuru T., Journal of The Electrochemical Society 156 (2009) C253-C258.

[28] Dam V.a.T., de Bruijn F. a., Journal of The Electrochemical Society 154 (2007) B494

[29] Borup R. *et al*., Chemical Reviews 107 (2007) 3904-3951.

[30] Mutsushuma S., Kawahara S., Ota K., Kamiya N., Journal of The Electrochemical Society 154 (2007) B153-B158.

[31] Inzelt G., Berkes B., Kriston Á., Electrochimica Acta 55 (2010) 4742-4749.

[32] Wang X., Kumar R., Myers D.J., Electrochemical and Solid-State Letters 9 (2006) A225.

[33] Benke G., Gnot W., Hydrometallurgy 64 (2002) 205-218.

[34] Conway B.E., Progress in Surface Science 49 (1995) 331-452.

[35] Jerkiewicz G., Vatankhah G., Lessard J., Soriaga M.P., Park Y.-S., Electrochimica Acta 49 (2004) 1451-1459.

[36] Ferreira P.J., la O' G.J., Shao-Horn Y., Morgan D., Makharia R., Kocha S., Gasteiger H.A., Journal of The Electrochemical Society 152 (2005) A2256.

[37] Ofstad A.B., Thomassen M.S., Gomez de la Fuente J.L., Seland F., Møller-Holst S., Sunde S., Journal of The Electrochemical Society 157 (2010) B621.

[38] Yadav A.P., Nishikata A., Tsuru T., Electrochimica Acta 52 (2007) 7444-7452.

[39] Speder J., Effect of Potential Cycling on Platinum Electrocatalysts in the Presence of Chloride Anions, University of Southern Denmark, 2010.

[40] Collette F.M., Lorentz C., Gebel G. & hominette F., J. Membr. Sci. 330 (1-2), 21-29, 2009.

[41] Huang X., SOlasi R., Zou Y., Feshler M., Reifsnider K., Condit D., Burlatsky S., Madden T., Journal of Polymer Science Part B : Polymer Physics 44 (16) (2006) 2346-2357

[42] Panha K., Fowler M., Yuan X.-Z., Wang H., Applied Energy, June (2011)

[43] Gittleman, C.S., Lai Y., Miller D.P., "Durability of Perfluorosulfonic Acid Membranes for PEM Fuel Cells", Honeoye Falls, NY, USA

[44] United States Department of Energy (DOE), Fuel Cells, March (2007) 1-8

[45] Sethuraman V.A., Weidner J.W., Haug A.T., Protsailo L.V., Journal of the Electrochemical Society 155 (2008) B119-B124

[46] Mathias M.F., Makharia R., Gasteiger H:A., Conley J.J., Fuller T.J., Gittleman C.J., Kocha S.S., Miller D.P. Mittelsteadt C.K., Xie T., Yan S.G., Yu P.T., The Electrochemical Society Interface (2005) 24-35

[47] http://www1.eere.energy.gov/hydrogenandfuelcells/pdfs/htmwg_benjamin.pdf (slide 8)

8. ABBREVIATIONS

BoL	Beginning-of-Life
BoP	Balance-of-Plant
CCB	Catalyst Coated Backing
CCM	Catalyst-Coated Membrane
CHP	Combined Heat and Power
DMFC	Direct Methanol Fuel Cell
EoL	End-of-Life
FC	Fuel Cell
GDL	Gas Diffusion Layer
HT	High Temperature
LSQ	Least SQuare
LT	Low Temperature
M	Project month e.g. M9 Project month 9
MEA	Membrane Electrode Assemblies
MS	MileStone e.g. MS1.2 meaning milestone no.2 in WP1
OCV	Open Cell Voltage
PEM	Proton Exchangeable Membrane
PTFE	Polytetrafluoroethylene (Teflon)
QA	Quality Assurance
SoA	State-of-the-Art
WP	Work Package
XRD	X-ray Diffraction